Chapter 7
Micro-XRF Core Scanning in Palaeolimnology: Recent Developments

Sarah J. Davies, Henry F. Lamb and Stephen J. Roberts

Abstract Within the last ten years, micro-XRF (μXRF) core scanning has become an important addition to the suite of techniques for investigating lacustrine sediments. Most studies to date have focused on records of detrital material. These have typically used elements such as Si, K, Ca, Ti, Fe, Rb, Sr and Zr as single element profiles or ratios. Inferences are made about changing catchment dynamics such as glacier advance and retreat, variations in run-off and soil erosion, weathering rates and processes and grain-size fluctuations. These can be linked, depending on the context of the individual basin, to factors such as climatic variability, meteorological events, seismic activity, tephra deposition or anthropogenic disturbance such as agriculture or deforestation. Studies of in-lake dynamics focus on elements affected by redox changes (e.g., Fe, Mn) or those which can be produced authigenically either as a result of evaporative concentration or biological processes (e.g., Ca). Here, we review the use of μXRF core scanning on lake sediments and summarise the range of elements and ratios that have been applied as a reference point for users. We consider some of the challenges involved in interpreting elemental data, given the wide variety of internal and external factors that can affect lake sediment composition.

Keywords Lake sediments · Palaeolimnology · XRF core scanning · Environmental proxies · In-lake processes · Flood histories · Varves

Introduction

The development of μXRF core scanning since the 1990s (see Rothwell and Croudace, this volume) has enabled rapid, non-destructive and high-resolution geochemical analysis of sediment cores. The first studies focused on marine sediments, building

S. J. Davies (✉) · H. F. Lamb
Department of Geography and Earth Sciences, Institute of Geography, History, Politics and Psychology, Aberystwyth University, Aberystwyth SY23 3DB, UK
e-mail: sjd@aber.ac.uk

S. J. Roberts
British Antarctic Survey, High Cross, Madingley Road, Cambridge CB3 0ET, UK

I. W. Croudace, R. G. Rothwell (eds.), *Micro-XRF Studies of Sediment Cores*,
Developments in Paleoenvironmental Research 17, DOI 10.1007/978-94-017-9849-5_7

upon the routine use of shipboard core scanning techniques for initial characterisation of physical properties. Since the arrival of a new generation of core scanners in the last decade (e.g., Croudace et al. 2006; Richter et al. 2006; for a recent overview, see Rothwell and Croudace, this volume), application of the technique to lake sediments has accelerated, with a notable rise in publications in the last five years.

Lake sediments are important terrestrial records of environmental change over a range of timescales, recording both catchment-scale dynamics and regional climatic variability (e.g., Cohen 2003). They can provide long, continuous and high-resolution archives comparable to those from oceans and ice cores. μXRF scanning has opened up new opportunities for the analysis of lake sediments, due to the range of elements that can be analysed, the high spatial resolution (up to 60 μm on some systems) and speed of analysis (Francus et al. 2009). This technological progress has occurred alongside efforts to standardise procedures for the curation, description and analysis of lake sediment cores (e.g., Schnurrenberger et al. 2001; Schnurrenberger et al. 2003). The impetus to develop more consistent protocols came from international collaborative initiatives such as the Global Lake Drilling Programme (GLAD) and the International Continental Scientific Drilling Programme (ICDP). μXRF scanning is now incorporated into the standard suite of initial palaeolimnological analyses applied to ICDP cores. With an increasing number of commercially available scanners in operation, access to facilities is also becoming more feasible for smaller scale projects.

In this paper, we examine how μXRF scanning of lake sediments has been used to interpret past environmental and climatic changes, often as part of broader multi-proxy investigations. The principal focus here is on the application of the technique. Issues relating to instrument configuration, sample preparation and data analysis are discussed in detail elsewhere by others (e.g., Tjallingii et al. 2007; Weltje and Tjallingii 2008; Boyle et al., this volume; Cuven et al., this volume; Jarvis et al., this volume; Rothwell and Croudace, this volume; Schillereff et al. 2014, although we do consider these issues where appropriate. First, we discuss the composition of lake sediments and consider the key elements and ratios in use and their environmental interpretation. We then discuss the use of μXRF core scanning in the characterisation of sediments and the development of core chronologies. We review the application of μXRF scanning across the spectrum of palaeolimnological research, including analysis of flood histories (e.g., Czymzik et al. 2013; Schillereff et al. 2014) and other 'event' deposits such as landslides, turbidites, seismites and lahars (e.g., Van Daele et al. 2014). We examine how μXRF scanning has contributed to the development of palaeoclimate records from lake sediments, such as long records of Quaternary climate variability (e.g., Scholz et al. 2007; Haberzettl et al. 2009; Melles et al. 2012), identification of rapid, abrupt climate shifts (e.g., Kylander et al. 2011; Lauterbach et al. 2011) and inter-annual climate variability (e.g., Metcalfe et al. 2010; Yancheva et al. 2007). We also discuss how μXRF can provide records of anthropogenic environmental changes such as catchment disturbance and metal pollution (e.g., Guyard et al. 2007; Niemann et al. 2013). Finally, we consider progress to date and discuss some potential future developments for μXRF scanning in palaeolimnological research.

Interpretation of XRF Scanning Data from Lake Sediments

Lakes and their catchments vary enormously in their physical, chemical and biological characteristics. The complexity of responses to within-lake and catchment processes leads to a highly diverse range of sediment types (Schnurrenberger et al. 2003). Therefore, a multi-proxy approach is required to disentangle the various factors that influence sediment composition and thus environmental interpretation. Geochemical analysis has historically been an important component of multi-proxy palaeolimnological reconstructions (Boyle 2001). Comprehensive reviews of geochemical methods and interpretations by Engstrom and Wright (1984) and Boyle (2001) built on earlier work by Mackareth (1966) and are key reference texts for researchers. In both, it is argued that chemical analysis of lake sediments is best used as a supporting technique, as interpretation can be less certain when parallel biological methods are not applied (Boyle 2001).

With the development of μXRF core scanners, high-resolution, continuous, multi-element datasets (typically in the range of atomic numbers Al–U, but some scanners can detect Mg) have become straightforward and relatively rapid. The general capability and speed has revolutionised the possibilities for the analysis of long cores and finely laminated sediments, where previously, detailed investigation of complete sequences using conventional destructive methods would have taken many months, or even years. Continuous datasets are also suitable for the application of time series analysis (subject to appropriate chronological control to ensure equal time intervals). The degree of cyclicity in observed variations and changes in system behaviour over time can be identified. These factors have led to a distinct increase in the prominence of elemental analysis in palaeolimnology over the last 5–10 years.

Influence of Lake Sediment Composition on Element Detection and Interpretation

Lake sediment composition is typically much more variable than that of marine sediments. The greater influence of catchment source area in most cases means that any changes on land are then transmitted to lake sediments. Abrupt boundaries between stratigraphic units are common, such as those at the Last Glacial-Interglacial Transition in deglaciated environments. Significant changes in water and organic content (higher and more variable than in marine sediments) require careful consideration when interpreting core scanning data (see Boyle et al., this volume). Detection of lighter elements is affected by the sediment water content (Tjallingii et al. 2007; Boyle et al. in Chap. 14), so downcore changes in the raw elemental counts may be caused by organic and water content variations, unrelated to sediment geochemistry. This was demonstrated by Elbert et al. (2012) in varved sediments from Lago Plomo in Argentina. Here, a decline in Si (from c. 8000 to 4–5000 counts per second

(cps)) and Ca (from c. 6500 to 5000 cps) in the top 25 cm of the core, is interpreted as an artefact of the increase in water content from c. 35 to 60%.

To counter these closed sum effects, and to avoid spurious patterns and relationships between elements, normalisation of raw data (peak area or cps) is increasingly commonplace. Weltje and Tjallingii (2008) proposed that data should be plotted as logarithmic ratios of element intensities, rather than as raw peak area cps data. Peak area element profiles are often normalised by the incoherent scatter (equivalent to Compton scattering) or total scatter (incoherent + coherent (Rayleigh) scatter) to minimise the effects of organic matter and water content (e.g., Guyard et al. 2007; Marshall et al. 2011; Kylander et al. 2011; Berntsson et al. 2014; Shala et al. 2014) or by the total counts at each depth interval (e.g., Cuven et al. 2011).

Löwemark et al. (2011) suggested normalising raw peak area data against Al to account for varying organic content, but noted that Al counts from core scanners can sometimes be too low to be effective. Nevertheless, normalisation by elements such as Al and Ti, both of which are abundant and stable, has been undertaken (e.g., Shala et al. 2014). For Al, comparatively poor detection limits require long dwell times to achieve reliable data, and in certain sediments, particularly organic-rich matrices, can be unachievable (Löwemark et al. 2011). Rubidium (Rb), being chemically similar to K, is often enriched in clay deposits. In minerogenic sediments where clay input remains relatively abundant and stable, Rb can be used as a normalising element in a similar manner to Al. Zr is more commonly abundant in some sediments and, advantageously, zirconium minerals (zircon) are resistant to weathering. However, Zr tends to be more concentrated in sand-size sediments and, therefore, is not suitable for use in normalisation, but is more useful as a proxy for variations in grain-size.

An alternative approach to removing the influence of water is by impregnating sediment blocks in resin before undertaking μXRF scanning. Although time-consuming, it is appropriate when high-resolution microfacies analysis of very finely-laminated sediments and/or varve counting are required (e.g., Van Daele et al. 2014).

An important consideration is whether quantitative data are required, which can then be compared with records from other sites. Most studies to date have presented data as peak area/counts per second or as ratios. To produce data equivalent to dry mass concentrations, calibration is required using conventional geochemical analysis of the sediments (see Boyle 2001). Boyle et al. (this volume) propose correcting for downcore variations in water content either using a regression based on a calibration dataset of elemental data from dry samples or x-ray scattering data produced during scanning. If the focus of the study is on those elements which are well detected by core scanning and the main interest is in relative changes downcore, or initial sediment characterisation, then quantification may not be necessary (Boyle et al., this volume).

Notwithstanding the issues relating to closed sum effects outlined above, the application of μXRF scanning in palaeolimnology has led to the use of a range of elements and elemental ratios for core characterisation and environmental proxies. We have identified 49 elements and ratios applied in palaeolimnological investigations, summarised in Table 7.1. The elements, ratios and associated interpretations

presented in Table 7.1 should not be taken as universally applicable, as several elements play multiple roles depending on their individual chemistry and on varying lake conditions (Kylander et al. 2011). Careful consideration is required of the climatic setting, local geology and key sediment sources, lake type and land use history. Investigation of modern catchment and lake processes (e.g., deployment of sediment traps) and elemental and mineralogical analysis of catchment material should, wherever possible, be used to ascertain the most appropriate elements and ratios to focus on and underpin the palaeoenvironmental interpretations for any given lake basin.

Catchment Erosion Proxies

A key application of XRF core scanning is to identify changes in the relative amount and nature of material derived from the lake catchment. Indicators of detrital inputs include the lithogenic elements Al, Si, K, Ti, Fe, Rb and Zr, because they are geochemically stable, hosted by resistant minerals, and conservative in most geochemical environments (Boës et al. 2011). Ratios of K/Al, K/Ti and Rb/K can be used to investigate changes in weathering regimes (e.g., Brown 2011; Arnaud et al. 2012), because K, like all alkali elements, is relatively water-soluble, while Al and Rb are less mobile during mineral weathering (Clift et al. 2014). Changes in grain-size of allochthonous material found in lake sediments have been inferred from elemental ratios such as Fe/Ti (increase = smaller grain-size), Ti/K (increase = larger grain-size; Marshall et al. 2011). Higher values of Zr/Rb represent finer material because Rb adsorbs strongly to clay minerals, whereas Zr is more abundant in silts, containing heavy minerals such as zircon, but this ratio is less reliable in coarser silts and sands (Kylander et al. 2011). Al/Si may potentially be used as a proxy for grain-size, since clays are rich in Al and sands in Si (Clift et al. 2014), although issues relating to detection of lighter elements as described above need to be considered. The link between grain-size and geochemistry is catchment-specific and reconstructions should ideally be validated by either correlation with grain-size measurements on specific layers or through the analysis of sediment trap data (Schillereff et al. 2014).

The lithogenic element Titanium (Ti) is often used as a proxy for erosion and transport of silt and fine sand. It is commonly associated with silts, either as Fe–Ti-oxides or Ti-rich magnetites, occurring in Fe-rich clastic mineral particles (e.g., ilmenite, rutile, brookite, sphene). Downcore variation in Ti has arguably been the most widely used element in μXRF lake sediment studies. It is used both to produce single element profiles, but is also a valuable tool for normalisation as it is an unambiguous indicator of allochthonous inputs from the catchment (Cohen 2003). For example, the Ca/Ti ratio can be used to identify Ca derived from within-lake processes such as evaporative concentration or biogenic production, whilst Si/Ti is used as a proxy for biogenic silica productivity (Brown et al. 2007).

Ti often co-varies with Fe and magnetic susceptibility, but as Fe can be affected by redox conditions and diagenesis (Mackareth 1966; Engstrom and Wright 1984; Boyle 2001), Ti is regarded as a more reliable indicator of catchment inputs

Table 7.1 Elements and elemental ratios from μXRF core scanning data applied in palaeolimnological studies as identified from published literature. For a number of elements and ratios, there are various interpretations based on the site-specific context

Element or ratio	Environmental interpretation (higher values)	Example location	Example reference
Al	Flood/detrital layers	Lago Maggiore, Italy	Kämpf et al. 2012
	Detrital siliclastics (Flysch Zone)	Lake Mondsee, Austria	Lauterbach et al. 2011
Al/Si	Fine silt and clay layers	Lake Villarrica, Chile	Van Daele et al. 2014
Br	Increased biological productivity/organic content	Lake Dalgan, Taimyr Peninsula, Siberia	Fedotov et al. 2012
	Increased organic content	Shira Lake, Siberia	Kalugin et al. 2013
		Lake Teletskoye, Siberia	Kalugin et al. 2007
	Sea spray/increased storminess	Isla de los Estados, Tierra del Fuego	Unkel et al. 2010
ln (Br/Ti)	Increased salinity/ marine influence	Tatos Wetland, Mauritius	De Boer et al. 2014
Ca	Increased calcite precipitation/evaporative concentration	Lake Malawi, eastern Africa	Scholz et al. 2007; Brown 2011
	Endogenic calcite production + detrital carbonates	Chew Bahir, Ethiopia	Foerster et al. 2012
	Increased primary productivity	Lake Mondsee, Austria	Lauterbach et al. 2011
	Increased marine influence	East Lake, Cape Bounty, Canada	Cuven et al. 2011
	Increased allochthonous lithoclastic material	Heimerdalsvatnet, Lofoten, Norway	Balascio et al. 2011
	Tephra	Lago Castor/Laguna Escondida, Chile	Elbert et al. 2013
		Faroe Islands	Kylander et al. 2012
Ca/Fe	Increased pedogenic input	Lago Castor/Laguna Escondida, Chile	Elbert et al. 2013
Ca/Mg	Biochemical calcite precipitation	Lake Mondsee, Austria	Lauterbach et al. 2011
Ca/Si	Water temperature change, either colder due to presence of calcite derived from ikaite or warmer due to association with green alga *Phacotus lenticularis*	Lake Potrok Aike, Argentina	Jouve et al. 2013

Table 7.1 (continued)

Element or ratio	Environmental interpretation (higher values)	Example location	Example reference
Ca/Ti	Increased evaporative concentration	Lake Potrok Aike, Argentina	Haberzettl et al. 2007; 2009; Jouve et al. 2013
	In-lake carbonate precipitation	Les Echets	Kylander et al. 2011
	Biologically mediated calcite production	Southwest Greenland	Olsen et al. 2013
Ca/ΣTi, Fe, Al	Increased authigenic carbonate precipitation (drier conditions)	Lake Peten Itzá, Guatemala	Mueller et al. 2009
Cu/Rb	Copper pollution from mining	Lake Bramant, French Alps	Guyard et al. 2007
Fe	Clay rich layers in varved sediment	Cape Bounty, Canada	Cuven et al. 2010
	Detrital inputs, redox conditions (non-stationarity)	Les Echets	Kylander et al. 2011
	Fine silt, clay of volcanic origin	Lake Villarrica, Chile	Van Daele et al. 2014
	Tephra	Faroe Islands	Kylander et al. 2012
Fe/Mn	Reducing conditions	Lake Montcortès	Corella et al. 2012
		East Lake, Cape Bounty, Canada	Cuven et al. 2011
		Lake Potrok Aike	Haberzettl et al. 2007
Fe/Si	Fine silt and clay, volcanic origin	Lake Villarrica, Chile	Van Daele et al. 2014
Fe/Ti	Reducing conditions	Lake Prespa, Balkan Peninsula	Aufgebauer et al. 2012
	Reduction in grain-size	Lake Tana	Marshall et al. 2011
K	Increased detrital input	Lake Prespa, Balkan Peninsula	Aufgebauer et al. 2012
	Increased detrital input	Lago Enol	Moreno et al. 2011
	Flood layers	Lago Maggiore	Kämpf et al. 2012
	Drier conditions (physical > chemical weathering)	Chew Bahir, Ethiopia	Foerster et al. 2012
	Clay rich layers in varved sediments	Cape Bounty, Canada	Cuven et al. 2010
	Fine-grained detrital inputs	Les Echets, France	Kylander et al. 2011
	Tephra	Lake Ohrid, Balkans	Vogel et al. 2010
	Tephra	Faroe Islands	Kylander et al. 2012

Table 7.1 (continued)

Element or ratio	Environmental interpretation (higher values)	Example location	Example reference
K/Al	Illite/kaolinite ratio (physical > chemical weathering)	Lake Tanganyika, eastern Africa	Burnett et al. 2011
K/Ti	Increased physical relative to chemical weathering	Lake Bourget, France	Arnaud et al. 2012
	Identification of upper varve boundary	Cape Bounty, Canada	Cuven et al. 2010
Mg	Detrital dolomite	Lake Mondsee	Lauterbach et al. 2011
Mg/Ca	Authigenic carbonate precipitation	Zoñar Lake, Spain	Martin-Puertas et al. 2011
Mn	Detrital inputs	Lake Taravilla, Spain	Moreno et al. 2008
	Mn-enriched siderite layers	Lake Suigetsu	Marshall et al. 2012
	Oxygenation of bottom waters (lower lake level)	Les Echets, France	Kylander et al. 2011
	Tephra	Faroe Islands	Kylander et al. 2012
Mn/Fe	Oxygenation of water column	El-gygytgyn, Siberia	Melles et al. 2012
	Oxic conditions	Albion Ponds, Jamaica	Burn and Palmer 2014
		Lago Galvarne Bog, Tierra del Fuego	Unkel et al. 2008
Mn/Ti	Oxygenation of water column	Lake Chungara, Chile	Moreno et al. 2007
		Les Echets, France	Kylander et al. 2011
Nb/Ti	Erosion of carbonate-rich magma intrusion	Lake Loitsana, Finland	Shala et al. 2014
P	Nutrient enrichment	Lake Montcortès, Spain	Corella et al. 2012
Pb	Pollution from mining	Lake Bramant, France	Guyard et al. 2007
		Lake Windermere, UK	Miller et al. 2014
Rb	Detrital inputs	Shira Lake, Siberia	Kalugin et al. 2013
	Fine-grained detrital inputs	Les Echets, France	Kylander et al. 2011
	Tephra	Lake Bramant, France	Guyard et al. 2007
		Lake Prespa, Balkans	Damaschke et al. 2013
Rb/K	Increased chemical weathering	Lake Malawi, eastern Africa	Brown 2011
		Lake Tanganyika, eastern Africa	Burnett et al. 2011
Rb/Sr log (Rb/Sr)	Increased chemical weathering	Laguna Cascada, Isla de los Estados, Tierra del Fuego	Unkel et al. 2010
			Fernandez et al. 2013

Table 7.1 (continued)

Element or ratio	Environmental interpretation (higher values)	Example location	Example reference
S	Increased marine influence	Heimerdalsvatnet, Lofoten, Norway	Balascio et al. 2011
	Gypsum precipitation (evaporative concentration)	Albion Ponds, Jamaica	Burn and Palmer 2014
	Soil derived S from leaching	Lake Tanganyika, eastern Africa	Burnett et al. 2011
		Lake Petén Itzá, Guatemala	Hodell et al. 2012
		Southwest Greenland	Olsen et al. 2013
S/Ti	Presence of pyrite, increased organic matter	Lake Chungara, Chile	Moreno et al. 2007
Si	Coarse silt and sand	Cape Bounty, Canada	Cuven et al. 2010
	Flood layers	Lago Maggiore, Italy	Kämpf et al. 2012
	Increased detrital inputs	Zoñar Lake, Spain	Martin-Puertas et al. 2011
	Increased detrital inputs	Lake Tana	Marshall et al. 2011
	Increased clay and quartz content	Lago Enol, Spain	Moreno et al. 2011
Si/Ti	Increased biogenic silica (principally diatoms)	Lake Malawi, eastern Africa	Brown et al. 2007; Brown 2011
		Lake Tanganyika, eastern Africa	Burnett et al. 2011
		Heimerdalsvatnet, Lofoten, Norway	Balascio et al. 2011
		Les Echets, France	Kylander et al. 2011
		Meerfelder Maar	Martin-Puertas et al. 2012
		El'gygytgyn, Siberia	Melles et al. 2012
		Laguna de Los Anteojos, Venezuela	Stansell et al. 2010
	Grain-size (sand)	Lake Loitsana, Finland	Shala et al. 2014
Si/Zr	High biogenic silica content relative to detrital material	East Lake, Cape Bounty, Canada	Cuven et al. 2011
Sr	In-lake $SrCO_3$ precipitation	Albion Ponds, Jamaica	Burn and Palmer 2014
	Erosion of granodiorite	Laguna Queshquecocha	Stansell et al. 2013
	Tephra	Lake Ohrid, Balkans	Vogel et al. 2010
Sr/Ca	Authigenic carbonate precipitation	Zoñar Lake, Spain	Martin-Puertas et al. 2011

Table 7.1 (continued)

Element or ratio	Environmental interpretation (higher values)	Example location	Example reference
Sr/Rb	Unweathered terrestrial fraction	Taimyr Peninsula, Siberia	Fedotov et al. 2012
		Teletskoye Lake, Siberia	Kalugin et al. 2007
Sr/Ti	In-lake $SrCO_3$ precipitation	Les Echets, France	Kylander et al. 2011
	In-lake $SrCO_3$ precipitation	Lake Chungara, Chile	Moreno et al. 2007
	Silt influx	Lake Loitsana, Finland	Shala et al. 2014
Th	Leaching of Th from soil during thawing of permafrost	Taimyr Peninsula, Siberia	Fedotov et al. 2012
Ti	Increased run-off/ rainfall	Laguna de Juanacatlan, Mexico	Metcalfe et al. 2010
	Increased run-off/ rainfall	Lake Montcortès, Spain	Corella et al. 2012
	Increased detrital input	Heimerdalsvatnet, Lofoten, Norway	Balascio et al. 2011
	Detrital input (glacier advance)	Laguna Lutacocha, Peru	Stansell et al. 2013
	Fine grained detrital input	Meerfelder Maar, Germany	Martin-Puertas et al. 2012
	Increased inwash of silt	Les Echets, France	Kylander et al. 2011
	Identification of flood layers	Lake Vuoksjávrátje, Sweden	Berntsson et al. 2014
	Increased glacial meltwater	Lake Ammersee, Switzerland	Czymzik et al. 2013
	Increased aeolian deposition	Lake Kråkenes, Norway	Bakke et al. 2009
	Silt-rich facies	Huguang Maar, China	Yancheva et al. 2007
	Clay-rich sediment	Cape Bounty, Canada	Cuven et al. 2010
	Tephra	Faroe Islands	Kylander et al. 2012
Ti/Ca	Increased detrital input	Lake Van, Turkey	Litt et al. 2009
Ti/K	Increased grain-size	Lake Tana	Marshall et al. 2011
Zr	Coarse silt and sand	Cape Bounty, Canada	Cuven et al. 2010
	Detrital inputs	Lake Tana	Marshall et al. 2011
	Tephra	Lake Ohrid, Balkans	Vogel et al. 2010
	Erosion of metasediments	Laguna Queshquecocha	Stansell et al. 2013
Zr/Fe	Flood layers/grain-size	Lake Blanc, France	Wilhelm et al. 2013
Zr/K	Coarser grain-size	East Lake, Cape Bounty, Canada	Cuven et al. 2011

Table 7.1 (continued)

Element or ratio	Environmental interpretation (higher values)	Example location	Example reference
Zr/Rb	Coarser grain-size	Lake Kumphawapi, Thailand	Chawchai et al. 2013
		Les Echets, France	Kylander et al. 2011
Zr/Ti	Weathered volcanic ash (catchment inwash)	Lake Malawi, eastern Africa	Brown et al. 2007
	Silt influx	Lake Loitsana, Finland	Shala et al. 2014
Inc/Coh	Higher values = increased organic content	Lake Bramant, French Alps	Guyard et al. 2007
		Lake Tanganyika, eastern Africa	Burnett et al. 2011
		Lake Potrok Aike, Argentina	Jouve et al. 2013

(e.g., Metcalfe et al. 2010). There are two main environmental interpretations of Ti which represent contrasting inferences about climate change. Higher Ti values could result from catchment run-off, indicating wetter conditions (e.g., Haberzettl et al. 2005, 2007; Metcalfe et al. 2010), but in some settings it may also indicate enhanced aeolian deposition (e.g., Yancheva et al. 2007; Kienel et al. 2009). Where catchment characteristics have been dramatically altered through time by climate change, it is possible that the major transport mechanism for Ti has changed. This is a particular issue with longer records, such as those spanning glacial-interglacial cycles and in arid areas, where lakes more readily dry out. Establishing covariance across multiple elements and supporting evidence via multiple proxies can help to establish whether the hydrological regime has sufficiently altered to affect the nature of the Ti record. Other factors influencing Ti flux include agricultural activities in the catchment and short-lived peaks in Ti may be related to tephra deposition. The problem of equifinality is by no means confined to interpretation of Ti profiles, but illustrates the importance of a detailed understanding of local catchment processes affecting the lake, regional climatic context and supporting evidence from other proxies. The use of correlation matrices for individual stratigraphic units (e.g., Kylander et al. 2011) can help to identify downcore changes in proxy relationships.

Foerster et al. (2012) highlight the need to understand the local basin context in their investigation of a c. 45 ka record from Chew Bahir, Ethiopia. Of the six elements (K, Fe, Si, Ti, Ca, Sr) that demonstrate a clear palaeoenvironmental signal (Fig. 7.1), they argue that K is the most reliable indicator of moisture fluctuations. During arid phases with relatively low vegetation cover, K-rich gneisses in alluvial fans on the western slopes of the basin would be readily eroded in a more irregular but intense rainfall regime. When the terrain is stabilised by more extensive vegetation cover, K would be preferentially leached away through chemical weathering, resulting in lower K values. K values are lowest during the interval corresponding to the 'African Humid Period' (~15–5 cal ka BP) punctuated by higher K values representing drought conditions during the Younger Dryas chronozone (Foerster et al. 2012).

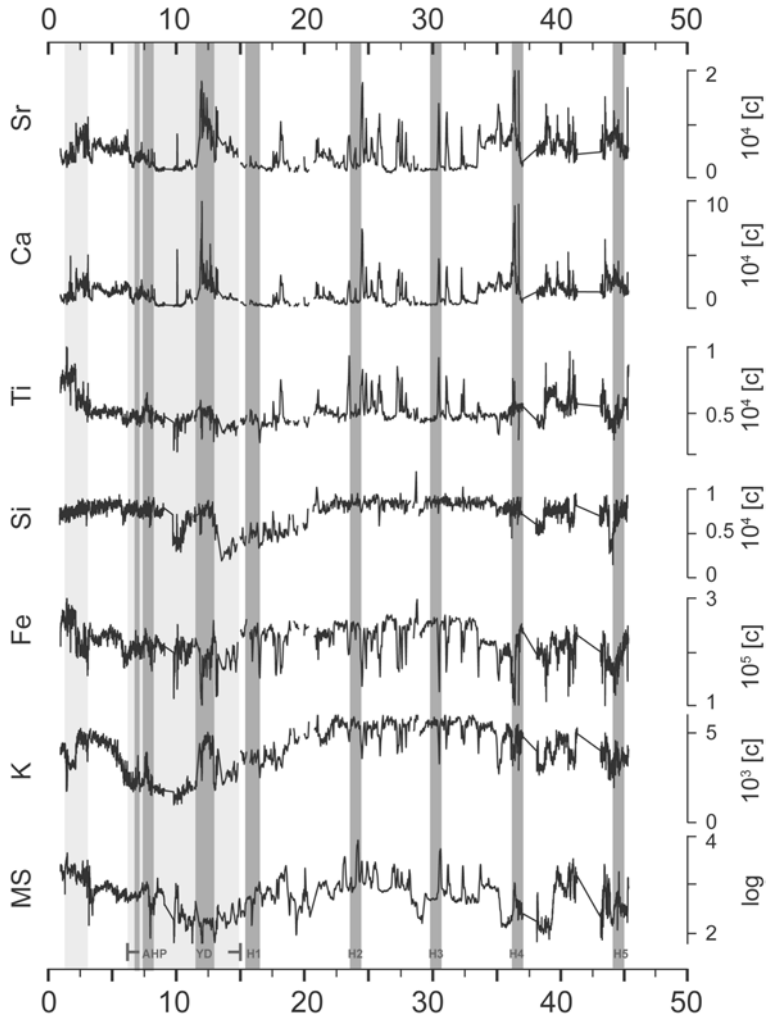

Fig. 7.1 µXRF data (in counts per second) from Chew Bahir, Ethiopia against time (cal ka BP). The *light grey shading* represents the African Humid Period (AHP), interrupted by the Younger Dryas (*dark grey shading*). (Reprinted from Quaternary International 274, Foerster et al. (2012), with permission from Elsevier.)

Proxies for In-Lake Processes

Within-lake responses to climatic and environmental change can also be identified using XRF scanning. During drier climatic episodes, lake levels decline, leading to the deposition of evaporative minerals. Eugster and Hardie (1978) described multiple pathways of brine evolution of lake waters which are dependent on the initial composition of fresh water, related to the underlying geology. Common evaporative minerals are $CaCO_3$ (calcium carbonate) and $CaSO_4$ (gypsum). XRF profiles of Ca (e.g., Scholz

et al. 2007; Mueller et al. 2009; Brown 2011) and S (Hodell et al. 2012) have been used to identify deposition of these minerals in lake sediment records (Table 7.1).

Iron (Fe) and manganese (Mn) profiles can provide information about changing redox conditions (Davison 1993). If lake waters are well-mixed, the water column remains oxygenated at depth. Anaerobic conditions at the sediment-water interface generally occur when lake waters are thermally and chemically stratified. Deeper lakes may remain stratified for extended periods, but generally, overturning of lake waters occurs on a seasonal/annual basis. Redox conditions can be affected by a range of factors, including changes in water depth, biological productivity, rapid sediment deposition as well as climatic drivers such as temperature, rainfall and wind regime. In a reducing environment, the solubility of Fe and Mn increases, but Mn is more readily affected (Boyle 2001), so an increase in Fe/Mn ratios can indicate the onset of anaerobic conditions. A shift to higher Fe/Mn may therefore point to a lowering of bottom-water oxygen content during enhanced stratification, or to de-oxygenation from organic decay following enhanced biological productivity linked to changing nutrient input. For example, at Lake Potrok Aike in Patagonia, low Fe/Mn ratios are interpreted to indicate increased lake mixing, either as a result of lower lake levels or increased wind speed (Haberzettl et al. 2007). At Lake Montcortes in northeast Spain, changes in aquatic productivity resulting from agricultural run-off is inferred from variations in Fe/Mn (Corella et al. 2012). As both Mn and Fe can also be derived from the surrounding catchment, normalising to Ti can help to establish the importance of redox processes relative to catchment inputs (e.g., Moreno et al. 2007; Kylander et al. 2011).

Sediment Characterisation

Along with traditional methods of identifying key components of lake sediments and other scanning methods, such as multi-sensor core logging (which generates magnetic susceptibility, gamma-density and p-wave velocity data), μXRF scanning is particularly valuable for rapid identification and correlation of stratigraphic units within a single basin. Simple statistical analysis can reveal which elements are consistently present and constantly contribute to >95% or >99% of total elemental counts. Usually, a combination of elevated values of 'measureable' lithogenic elements (e.g., Al, Si, K, Ti, Fe, Rb, Zr) can be used to characterise clastic sediments, although Fe can be influenced by redox processes and Si can reflect biogenic deposition (Brown, this volume). The presence of Ca and Sr is commonly associated with authigenic carbonate minerals or biogenic calcium carbonates in arid and limestone/carbonate environments, but can be covariant with lithogenic elements in volcanic and/or glacial environments when derived from catchment inwash, aeolian activity, and/or soil development in the catchment (Sr). The use of ratios can help to clarify the key processes governing downcore variations. For example, Mueller et al. (2009) used the ratio of Ca/Σ (Al, Ti, Fe) to help identify a period of enhanced authigenic carbonate deposition in sediments from Lake Peten Itza, Guatemala between 4.5 and 3.5 cal ka BP. However, it is important to ascertain that as far as possible that the factors controlling observed geochemical changes remain consistent.

μXRF scanning can be used to make inferences about the biological component of lake sediments. Si/Ti has been used to estimate biogenic silica (Brown et al. 2007; Brown, this volume; Stansell et al. 2010), where high values represent enhanced productivity. Biogenic silica usually represents diatom productivity as the silica frustule of the algae is preserved in lake sediments, however there may also be contributions from chrysophytes and sponges. A potential allochthonous source of biogenic silica comes from grass phytoliths, which may be significant in some nearshore contexts. Ca values may also reflect biogenic calcium carbonate productivity, although this may be difficult to distinguish from calcite precipitation resulting from evaporative concentration without more detailed examination of the sediment.

XRF scanning data has also been used as a proxy for organic content of lake sediments. One of the most commonly used parameters is the incoherent/coherent (inc./coh.) scattering ratio (e.g., Guyard et al. 2007; Brown et al. 2007; Burnett et al. 2011). This ratio is an approximation of the atomic number of the average matrix composition. In wet sediments, most of the scatter is produced by X-ray interactions with elemental carbon and water (inc) and water (coh), whose elements (H, C, O) are not detectable by XRF. Since organic carbon has a lower average atomic number than silica, carbonates or any clastic material, increased organic content can be inferred qualitatively from higher inc/coh ratios (e.g., Burnett et al. 2011). This x-ray back scattering data (coh./inc. ratio) can also be used to account fluctuations in water content. Boyle et al., this volume demonstrate that the coh./inc. ratio can be used to convert wet concentration data to a dry mass basis, the method being particularly suited to cores with large variations in water content.

Moreno et al. (2007) suggested that S/Ti ratios may be a useful proxy for organic matter in Lake Chunagara, Chile, where higher S/Ti values corresponded to increased Total Organic Carbon (TOC). They proposed that this is due to increased pyrite formation in organic sediments, but caution that microscopic examination of sediments is also required, due to some very low values of S (Moreno et al. 2007). Bromine (Br) has also been proposed as a potential tool for identifying relative changes in organic content in lake sediments e.g., Kalugin et al. 2007) as Br forms strong covalent bonds with organic molecules (Gilfedder et al. 2011). In their study of an 800 year annually laminated record from Lake Teletskoye Lake, Siberia Kalugin et al. (2007) found that Br measured by μXRF core scanning covaries with % TOC measurements. Analysis of the Br flux in Lake Constance, where Br was found to be permanently removed to the lake sediment, supports the use of Br as a proxy for past biological productivity (Gilfedder et al. 2011). It has also been suggested that excess Br in cores from sites exposed to maritime influences, may also be the result of enhanced storminess (Unkel et al. 2010; Turner et al. 2014). In a recent Holocene record from Mauritius, De Boer et al. (2014) use increased (ln) Br/Ti ratios to infer infiltration of saline groundwater into a low-lying coastal wetland. As with other elements, there are a range of potential interpretations depending on local site characteristics. Further investigation of Br as a reliable proxy is needed and any potential geological sources should also be considered.

After determining which elements are present and most abundant (and useful), another important first step for lacustrine μXRF scanning studies is to establish

which elements are covariant, and which relate closely to scattering parameters. Simple correlation coefficient analysis can rapidly highlight which elements are most readily aligned with lithogenic elements (e.g., Al, Ti, Fe, Rb, Zr) or more likely to be closely aligned to organic variability (as measured by incoherent and coherent scatter and/or %LOI, %TOC subsample data). Multivariate approaches have been used to reveal associations between elements and deviations that can be environmentally significant (e.g., PCA; Balascio et al. 2011; Shala et al. 2014). Whichever statistical method used, it is important to be aware that that covariance can change between units, be related to sampling interval, and some elements, commonly Fe and Mn can change according to a combination of these factors.

Applications of µXRF Scanning

Flood Histories

A significant development in µXRF scanning has been the identification of flood layers and the reconstruction of flood histories (e.g., Moreno et al. 2008; Czymzik et al. 2013; Schillereff et al. 2014, this volume). This approach is complementary to that applied to fluvial sedimentary sequences (e.g., Jones et al. 2010; Turner et al., this volume). For example, in their study of two varved cores covering the last c. 5500 years from the pre-Alpine Lake Amersee, Czymzik et al. (2013) identified 1573 detrital layers in either one or both sequences using Ti data and layer thickness. Three principal depositional units were identified: from 5500 to 2800 varve years BP; from 2800 to 400 varve years BP and from 400 varve years BP to present. Between 2800 and 400 varve years BP, detrital layers were thicker and deposited more regularly. A further increase in flood intensity was observed during the last 400 years. Comparison with the record of human occupation of the basin does not indicate a strong link between human activity and flood intensity, a conclusion supported by other studies of pre-Alpine lakes (e.g., Arnauld et al. 2012). Czymzik et al. (2013) argue that the observed changes in flood intensity can be explained by a combination of reduced influence of orbital forcing in the late Holocene combined with solar activity minima.

Moreno et al. (2008) constructed a 2000 year flood chronology from Lake Taravilla in the central Iberian range of northeastern Spain using a combination of physical sediment properties and XRF data. Principal component analysis of the XRF data revealed that Axis 1 is linked to carbonate inputs (Ca), whilst Axis 2 is related to siliclastic deposition (Si, K, Ti, Fe, Mn). Centimetre to decimetre scale terrigenous layers were characterised by coincident peaks in carbonate and siliclastic indicators, particle fining upwards within a layer, and by relatively high organic content, particularly at the base of the sequences. Similar to Czymzik et al. (2013) findings, increased flood activity occurred during the last few hundred years. Comparison with pollen records revealed no evidence of anthropogenic influence and again centennial scale reduction in solar activity is postulated as a key driver of

flooding. Moreno et al. (2008) also argue that the North Atlantic Oscillation plays a role in influencing decadal scale variability in flooding.

In their comprehensive review of palaeoflood records from lake sediments, Schillereff et al. (2014) highlight the types of lake most suited for preserving an archive of historical floods. They stress the need for a detailed knowledge of the local geology, catchment characteristics (e.g., basin morphology) and in-lake processes (e.g., stratification), which may affect the nature of sediment transport and deposition. The framework provided by Schillereff et al. (2014) for this process-based approach is a valuable tool for this growing area of palaeolimnological research.

Identifying the Location of Tephra Layers

There has been considerable interest in the potential of XRF scanning to assist in the location of tephra layers in sediment cores, including those which may not be easily found on visual inspection. For example, Vogel et al. (2010) examined the tephrostratigraphy of Lake Ohrid, on the Albania-Macedonia border, during the last glacial-interglacial cycle, using a combination of XRF scanning, magnetic susceptibility logging and visual inspection. Peaks in K, Zr and Sr relating to four visible tephras were used to help locate a further six tephra layers. Similarly, Damaschke et al. (2013) identified 11 tephra layers (including five 'cryptotephras') from nearby Lake Prespa in a record spanning at least the last c. 60,000 years, using in this case K, Rb and Sr. Moreno et al. (2007) found that peaks in Al, K, Ti and Fe were associated with tephra layers, along elements such as Zr, Sr, Sn and Ba. Tephras are not always easily distinguishable with XRF-scanning data. In their record from Laguna Cascada on Tierra del Fuego, Unkel et al. (2010) described two tephras in the core stratigraphy. One, at c. 8.5 cal ka BP, linked to Mt Hudson, is clearly marked by peaks in Ca, K, Ti, Zr and Sr, whilst the other at c. 4.5 cal ka BP, thought to originate from Mt Burney, visible in the sediments, does not exhibit a distinct geochemical signal. Wastegård et al. (2013) noted in a sequence from Potrok Aike, Patagonia, that tephra layers were often associated with a peak in K and a trough in Ti.

Kylander et al. (2012) examined the potential of XRF-scanning in tephrochronology. In their analysis of three sediment cores from the Faroe Islands, rhyolitic tephras in low shard concentrations ($<850/cm^3$) were not identified by μXRF scanning, whilst basaltic tephras present at more than 1000 shards per cm^3 were highlighted by peaks in Ti, Fe and Ca. Location of cryptotephras depends on whether sufficient shards are located near the core surface and can be detected. Kylander et al. (2012) concluded that whereas μXRF scanning can assist in highlighting areas for further detailed investigation and also in the identification of possible reworking, the elemental data cannot be a substitute for systematic microscopic examination and quantitative analysis of major and trace element geochemistry using conventional methods. In this volume, Balascio et al. take an experimental approach to characterising the signal from tephra layers. They also found that basaltic tephras had a distinctive geochemistry, different from the background matrix. It would be useful

to extend this type of study further by using tephras with a range of geochemical signatures set in a matrix of various sediment types.

Varved Sequences

Given the high sampling resolution of µXRF scanning, it is particularly suitable for the examination of finely laminated sediments and varved sequences (e.g., Neugebauer et al. 2012; Schlolaut et al. 2014). µXRF scanning data can help to identify clay and tephra layers that are geochemically distinct from the regular varves (Francus et al. 2009). At Meerfelder Maar in Germany, varves are characterised by couplets of two main components: a spring/summer layer consisting almost entirely of biogenic silica from diatom blooms and an autumn/winter layer of minerogenic, detrital material (Martin-Puertas et al. 2012). Here, a seasonally resolved record was produced from µXRF data, with high Si/Ti values representing increased diatom productivity and Ti reflecting detrital inputs. Increased Si/Ti values between 2 and 5 cal ka BP were interpreted to reflect enhanced water circulation from increased wind stress. Martin-Puertas et al. (2012) note that Ti, when compared with a pollen-based precipitation reconstruction, did not exhibit a clear relationship with precipitation after 5 cal ka BP. This is attributed to changes in lake morphology as a result of rising lake levels. A reduction in the amount of detrital material reaching the deeper parts of the basin due to greater distance from the inflow would have led to sediment being trapped in the delta. This example highlights the importance of considering non-stationarity of processes in the local catchment as an explanation for observed variations in elemental data.

Van Daele et al. (2014) distinguished four different 'event' deposits (lacustrine turbidites, tephra-fall layers, 'runoff cryptotephras', and lahar deposits) in cores taken from Lago Villarrica and Lago Calafquén in the volcanically and seismically active Chilean Lake District. This multi-proxy investigation was underpinned by an ultra-high-resolution record of volcanic activity determined by XRF scanning of resin-embedded sediment blocks. Si, Al and Fe ratios were used to distinguish between the three sedimentary components: diatom frustules (high Si), terrestrial clays (Al enriched), and mafic volcanic ash (elevated Fe) (Fig. 7.2). The c. 600-yr-old eruption history for the Villarrica Volcano contained in varved lake-sediment sequences from Lago Villarrica demonstrates that the Villarrica volcano has had, on average, a 22 year dormancy period for eruptions with a Volcanic Explosivity Index (VEI) >2. Although Villarrica is constantly active, and a relatively minor Strombolian eruption started in on 3rd March 2015, the last VEI>2 eruption from Villarrica was in 1991, 24 years ago.

Cuven et al. (2010) examined clastic varved sequences from two high Arctic lakes to determine their composition and investigate links between grain-size and chemical characteristics. They found distinct geochemical signatures associated with different grain-sizes. Coarse layers dominated by sand were found to have high values of Si and Zr, Ti was characteristic of silt layers and clay layers were associated with Fe and K. Varve composition was split into four principal lithozones

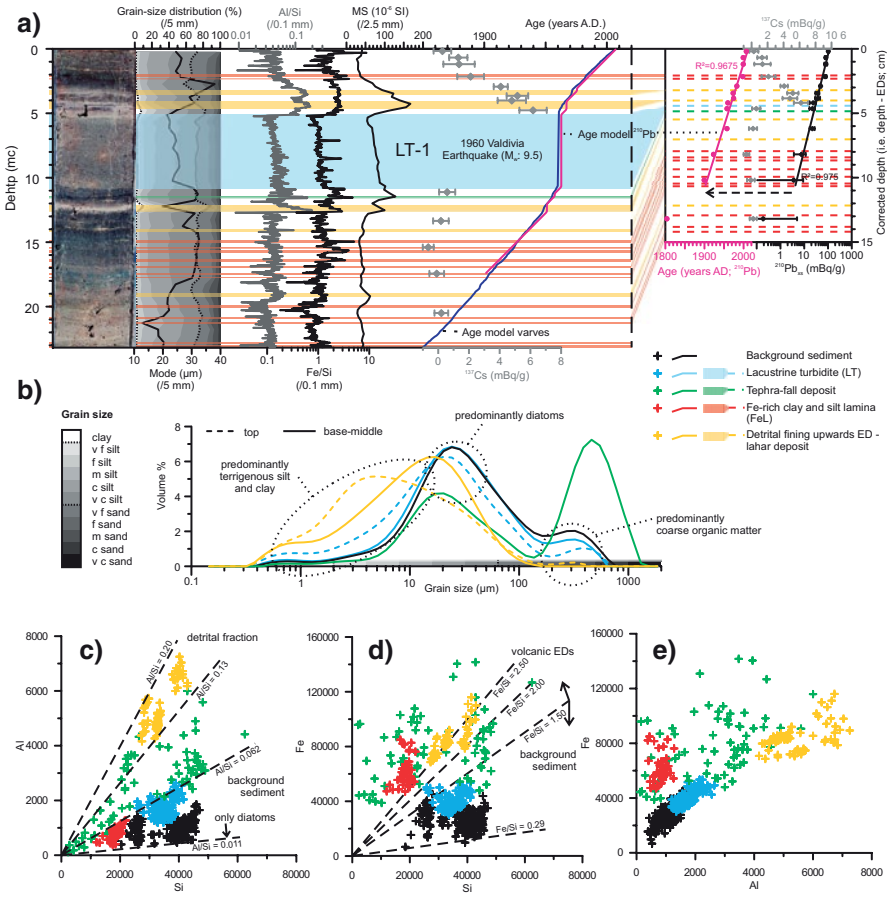

Fig. 7.2 **a** Core CAGC02bis from Lake Calafquén with grain-size distribution and ^{137}Cs (*grey diamonds*), ^{210}Pb (*pink line*) and varve (*dark blue line*) age-depth models for the last 150 years distribution, µXRF ratios, and magnetic susceptibility (MS). The four different types of event deposits are shown by coloured symbols; **b** Grain-size distribution of background sediment (*black*), tephra-fall deposits (*green*), and both base/middle (*solid*) and top (*dashed*) of detrital fining -upward event deposits (*yellow*) and lacustrine turbidites (*blue*); **c–e** Micro-XRF elemental counts in core CAGC02bis of Al versus Si (**c**), Fe versus Si (**d**), and Fe versus Al (**e**). *Dashed lines* represent elemental ratios differentiating between background sediment and event deposits. (Adapted from van Daale et al. (2014))

reflecting different depositional processes. For example, the silt layer grading into clay (Lithozone A) was interpreted to derive from spring snowmelt, whilst the coarser sediments of Lithozones B and C were indicative of higher intensity run-off episodes (Cuven et al. 2010). It was also found that K/Ti was a reliable indicator of the upper boundary of varves. The two examples here highlight the role µXRF scanning can play in identifying links between elemental data, grain-size and depositional processes. In non-varved sequences, understanding these relationships can be more challenging.

A major contribution of μXRF scanning to the development of sediment chronologies came through the Lake Suigetsu 2006 Varved Sediments Project (Marshall et al. 2012; Nakagawa et al. 2012; Bronk-Ramsey et al. 2012). Laminated sediments of sub-annual resolution at Lake Suigetsu, Japan, extend back c. 70,000 years. In addition to seasonal layers represented by a spring diatom bloom, an organic summer layer, a siderite-rich autumn layer and a clastic winter layer, the sediments also contain well-preserved leaf macrofossils throughout. The Suigetsu sequence therefore presented an unparalleled opportunity to extend and refine the radiocarbon calibration curve. A key element of the study was accurate varve counting, which was undertaken using two independent methods: μXRF scanning (Marshall et al. 2012) and microscopic varve counting (Schlolaut et al. 2012). Specially-developed and freely-available, software, Peakcounter (http://dendro.naruto-u.ac.jp/~nakagawa/), was used to count varves from multiple element data generated by μXRF scanning. Mn, Fe and Ti were the key indicators used to identify layer boundaries along with greyscale values obtained from X-radiography using an Itrax core scanner (Fig. 7.3). Repeat analyses at different x-ray tube power settings and count times demonstrated that settings of 30 mA and 30 kV, with a relatively short count time of 4 s, produced an appropriate signal to noise ratio for the elements of interest without compromising the quality required for varve identification.

Figure 7.3 illustrates how quality-classified counts were produced, with Qlt-1 assigned to the clearest signals in multiple indicators through to Qlt-4, assigned to low and indistinct peaks, such as those produced by poorly preserved and indistinct siderite layers (Marshall et al. 2012). For each step, errors were identified and quantified. The μXRF data compared well with the counts derived from microscope analysis and the two methods were combined to produce a single, robust chronology. This sequence formed the cornerstone of a new terrestrial radiocarbon calibration curve from 11.2–52.8 cal ka BP, which for the first time allows atmospheric calibration of radiocarbon dates into the last glacial period and to the limits of the dating method (Bronk Ramsey et al. 2012), representing a major development in Quaternary science.

Climate Variability Inferred from μXRF Scanning of Lake Sediments

In this section, we discuss the principal use of μXRF scanning to investigate past climate change. We examine records covering a range of timescales, from long records extending into the last glaciation and beyond, those which focus on the identification of rapid and abrupt changes and those which record high resolution variability over interannual timescales. The palaeoclimatic interpretation from geochemical profiles in lake sediments depends on the interplay between lake and catchment characteristics and the climatic regime and therefore may vary between sites and over time.

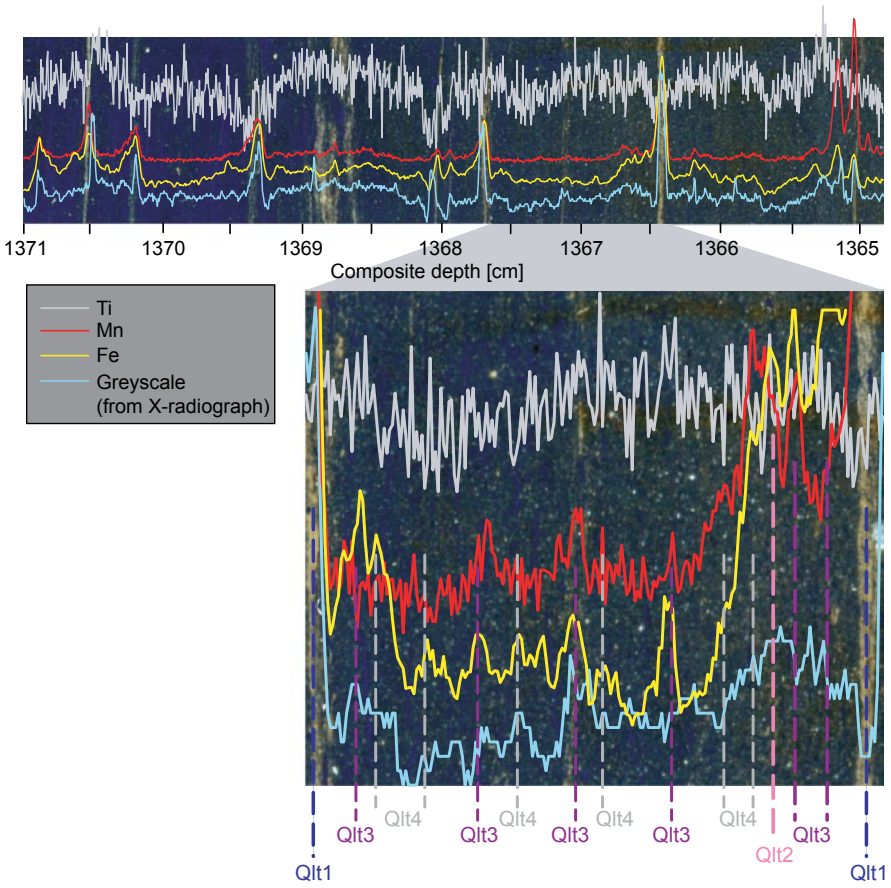

Fig. 7.3 Thin section photograph overlain with µXRF indicator elements and X-radiograph greyscale data from core BN-07, Lake Suigetsu. The enlarged sub-section demonstrates how quality counts (Qlt to 4) were derived. (Reprinted from Marshall et al. (2012), with permission from Elsevier)

Long Records of Climate Change

Some of the first published µXRF scanning data from lake sediments were obtained from Lake Malawi in eastern Africa (Brown et al. 2007; Scholz et al. 2007) and Laguna Potrok Aike in Patagonia (Haberzettl et al. 2005, 2007, 2009). Both projects were supported by the Global Lakes Drilling Program and the International Continental Scientific Drilling Program, with the aim of producing long palaeoclimatic sequences extending back through the last glacial cycle. Since these studies, µXRF scanning has been incorporated into the standard set of analyses for ICDP projects such as Lake Van in Turkey (Litt et al. 2009), Lake Ohrid in the Balkans (Vogel et al. 2010) and El'gygytgyn in Siberia (Melles et al. 2012).

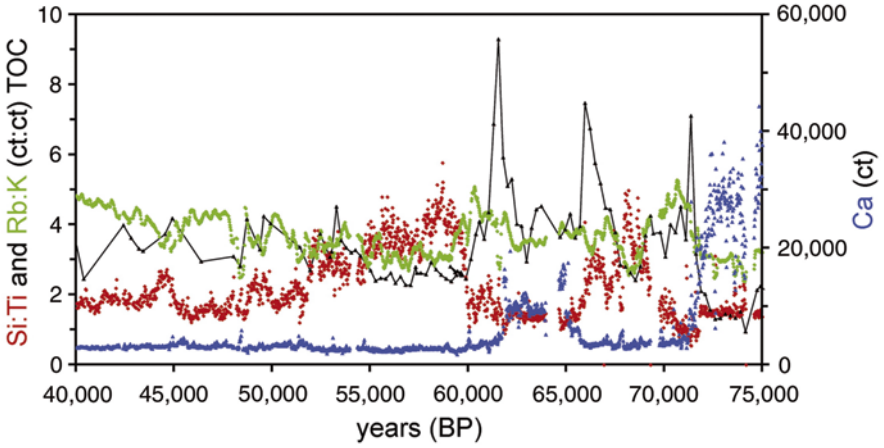

Fig. 7.4 Profiles of Si/Ti (biogenic silica), Rb/K (chemical weathering), Ca (calcite precipitation) and % TOC for Lake Malawi from 40 to 75 ka BP. (Reprinted from Brown (2011), with permission from Elsevier)

The sediments of Lake Malawi are arguably the most comprehensively studied in Africa (see Scholz et al. 2011). Cores obtained by the Lake Malawi Scientific Drilling Project in 2005 have provided important insights into tropical climate dynamics during the last glacial-interglacial cycle. Scholz et al. (2007) identified evidence of a dramatic change in the hydrological regime of Lake Malawi c. 75,000 years ago. Between 135 and 75 ka BP, the lake was characterised by major fluctuations in lake level indicated by the downcore Ca profile. Higher values of Ca suggest generally drier conditions, with several major excursions indicative of a series of 'megadroughts.' This interpretation was supported by seismic profiles revealing evidence of unconformities and more recent μXRF data from Lake Tanganyika (Burnett et al. 2011). After c. 70 ka BP, Ca values were greatly reduced indicating more humid conditions. It was suggested that climate may have played a role in the dispersal of modern humans after 70 ka BP, with wetter conditions creating a more favourable environment for migration (Scholz et al. 2007). Detailed investigation of the megadroughts, using μXRF scanning data, suggests that a complex pattern of process is recorded in the μXRF data (Fig. 7.4; Brown 2011).

The termination of droughts at 72 and 62 ka BP was characterised by increased inwash of organic matter (%TOC), quickly followed by the deposition of chemically weathered material (Rb/K) which had been stored on the catchment slopes during the arid phase. Subsequent exposure of fresh material led to an increase in weathering of bioavailable silica which stimulated periods of enhanced diatom productivity when washed into the lake (Brown 2011). More recently, Lane et al. (2013) examined Malawi sediments to determine whether the eruption of Mount Toba, Sumatra c. 75,000 years ago, had an impact on climate in eastern Africa. A tephra layer in the sediments at 28.08–28.10 m below lake floor was identified as

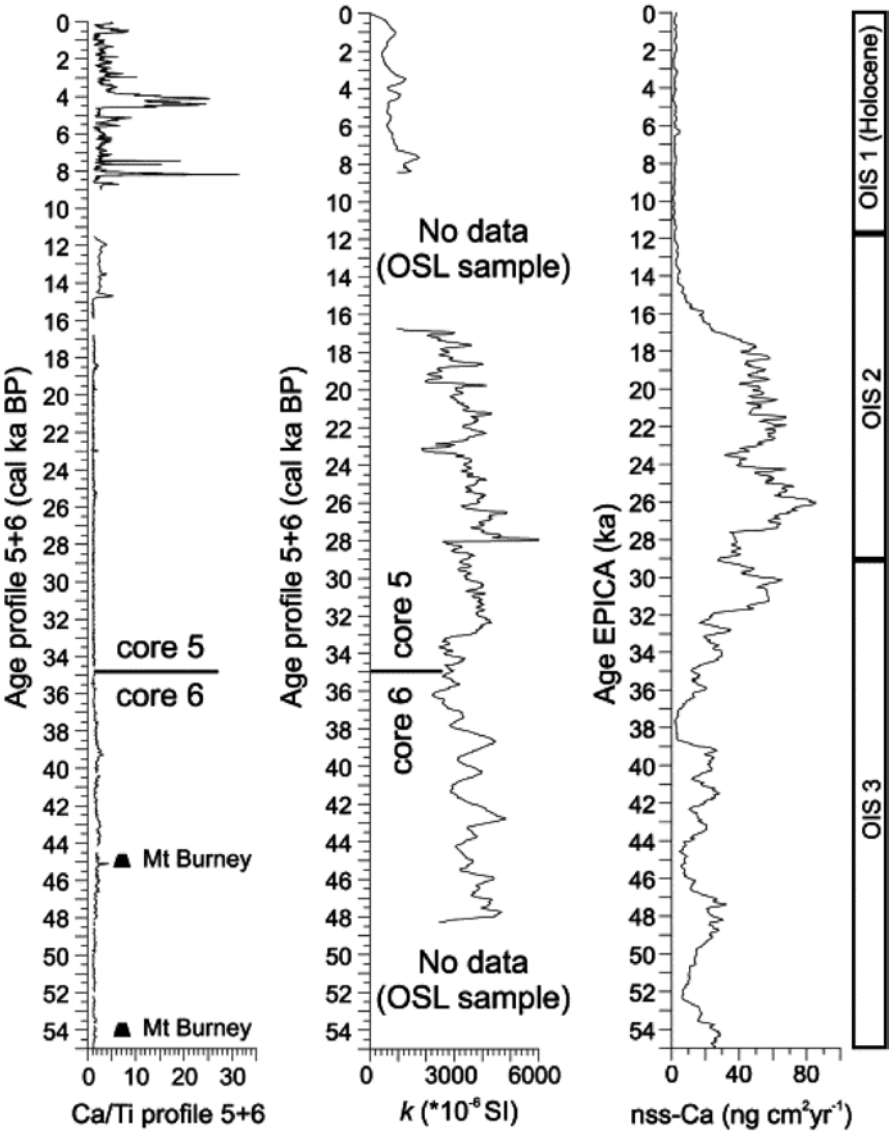

Fig. 7.5 The Ca/Ti record from a 55 ka sequence at Potrok Aike, Argentina, compared with magnetic susceptibility (*k*) smoothed with an 11 point moving average and non sea salt calcium (nss-Ca) flux from Dome C. Cores 5 and 6 are correlated using the older Réclus tephra layer. (Reprinted from Haberzettl et al. (2009), with permission from Elsevier)

the Younger Toba Tuff (YTT) using electron microprobe analysis. μXRF scanning data (Si/Ti; inc/coh; Zr/Ti) showed no major change in the sediments immediately above the tephra layer. Lane et al. (2013) concluded that the eruption of the YTT did

not have a significant climatic impact in eastern Africa and therefore could not be the cause of a genetic bottleneck in human populations at that time.

At Laguna Potrok Aike, Ca/Ti is interpreted as a proxy for lake level fluctuations during the last c. 55 ka BP (Haberzettl et al. 2009). The Ca/Ti profile indicates a substantial shift in hydrological conditions after c. 8 cal ka BP, with higher values suggesting a negative water balance and significant drought events at c. 8, 4 and c. 0.5 cal ka BP (Fig. 7.5). Much lower values between c. 12 and 55 cal ka BP suggest high lake levels (possibly overflowing) which may be due to reduced evaporation during glacial conditions rather than increased precipitation (Haberzettl et al. 2009). With a consistently positive water balance through this period, minor lake level fluctuations may not have been sufficient to induce significant authigenic carbonate precipitation. Ca/Ti is slightly elevated during the Lateglacial, between c. 15.8 and 11 cal ka BP, with higher values corresponding to the Younger Dryas chronozone (Haberzettl et al. 2007, 2009). However, more recent analysis by Jouve et al. (2013) suggest that the presence of micropumice in sediments between 15.2 and 11.8 cal ka BP compromises the integrity of the Ca/Ti record during this period. Micropumice was found to have lower Ti values, thus having an impact on its use as a proxy for detrital inputs and in normalisation. Jouve et al. (2013) argue that Si is a more appropriate normalising tool in this context as analysis showed that Si values reflected detrital inputs rather than biogenic silica (Nuttin et al. 2013).

Due to the high sampling resolution, μXRF scanning is ideally suited to identify abrupt changes in climate such as Heinrich events during the last glaciation. Kylander et al. (2011) examined the geochemical record from the Les Echets sequence in northern France, where previous research had revealed evidence for a response to Heinrich events in the palaeoecological record (Wohlfarth et al. 2008). Correlation matrices established that the relationships between elements changed through the core, related to the substantial changes in lake status evident from the stratigraphy and other proxies (Kylander et al. 2011). A consistent relationship was, however, observed between Ti, K and Rb, reflecting inputs from the catchment and presence of clay minerals. Geochemical data were used to explore changes in detrital inputs (Ti, K, Rb, Zr, Si), grain-size (Zr/Rb) and lake levels and aquatic productivity (Ca, Sr, Mn, Si), summarised in Fig. 7.6. A key finding from the μXRF profiles was that Heinrich events previously identified in the diatom record (low productivity) corresponded with periods of lower lake level. For example, at 31.2 ka BP, an increase in Ti and decrease in Zr/Rb point to more detrital inputs from fine-grained sources, which coupled with lower lake levels based on Sr, Mn and Ca data, indicate a greater influence of aeolian transport of material (Kylander et al. 2011). The duration of H events as defined by μXRF scanning (Ti = detrital inputs and Zr/Rb = grain-size) was shorter than that inferred from the diatom record. This study demonstrates the need to consider changes in proxy relationships through time, particularly in relation to stratigraphic units.

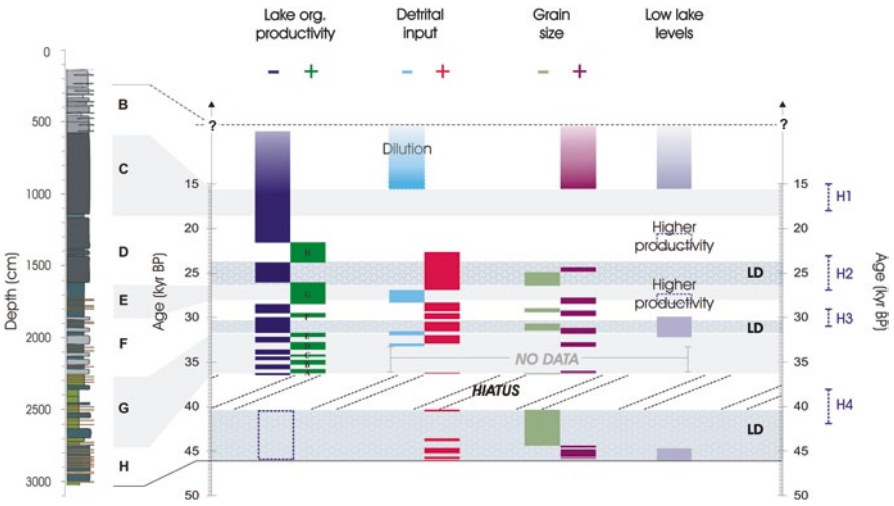

Fig. 7.6 Summary of the palaeoenvironmental interpretation from the Les Echets sequence, France, from c. 40 to 16 cal ka BP. Lake productivity is from Wöhlfarth et al. (2008), detrital inputs based on Ti data, grain-size is inferred from Zr/Rb and lake levels based on Sr, Ca and Mn μXRF data. (Reprinted with permission from Kylander et al. (2011))

Last Glacial-Interglacial Transition and Holocene

Rapid climate fluctuations during the last glacial-interglacial transition have been the subject of a number of studies involving μXRF scanning (e.g., Haberzettl et al. 2007; Bakke et al. 2009; Neugebauer et al. 2012). The resolution of the data enables comparison of the timing of responses of different locations to the major changes observed during deglaciation. For example, Stansell et al. (2010) using increased detrital inputs represented by Ti, identified a glacier advance at 12.85 cal ka BP at Laguna de los Anteojos, a cirque lake in the Venezuelan Andes. They established that maximum glacier extent occurred at 12.65 cal ka BP with deglaciation complete by 11.75 cal ka BP. The changes in the Ti profile are not as abrupt as those observed at higher latitudes, such as at Lake Kråkenes in Norway (Bakke et al. 2009; Stansell et al. 2010). It is argued that the early warming evident in Venezuela would have contributed to triggering warming in the northern high latitudes through the stimulation of a more vigorous hydrological cycle (Stansell et al. 2010).

Stansell et al. (2013) also used μXRF elemental profiles to investigate Holocene glacier fluctuations in the Peruvian Andes. They presented data from three sites, all of which show evidence of glacier advance between 8 and 4 cal ka BP through increased inputs from detrital material, bulk density and magnetic susceptibility. Here, knowledge of variations in the geochemical composition of catchment rocks was crucial to the interpretation of the XRF scanning data as the three catchments had slightly different downcore profiles. For example at Lake Queshquecocha, geochemical variations were observed at different elevations in the watershed as well

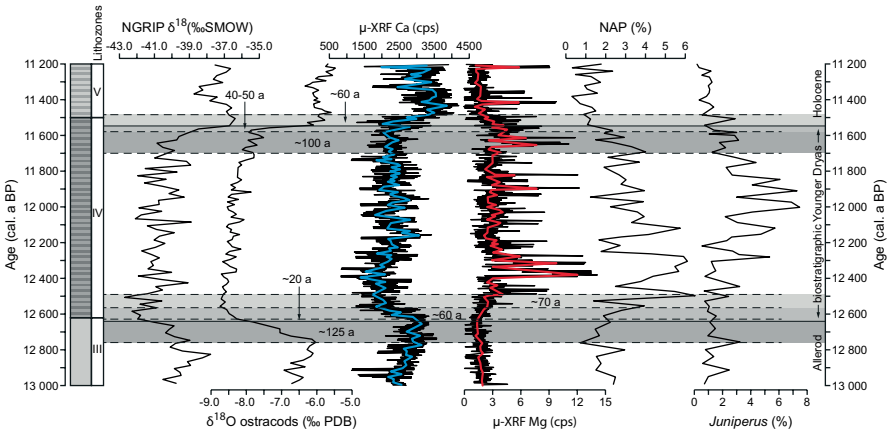

Fig. 7.7 Selected proxy data from Mondsee spanning the Allerod-Younger Dryas and Younger Dryas-Holocene transitions. *Grey shaded* areas represent major proxy responses and their approximate durations. The *red line* on the Mg profile is a 25 pt running mean. (Redrawn from Lauterbach et al. (2011))

as distinct signatures from till and moraine samples. Bedrock at the headwall had higher concentrations of Zr, whilst at lower elevations Sr and Ca were present at higher levels in the surrounding granodiorites. Increased levels of Sr and Ca in down core profiles were therefore indicative of catchment erosion at lower elevations, whilst Zr inputs increased as the glacier retreated back towards the headwall (Stansell et al. 2013).

At individual sites, the rates of response of different proxies to rapid environmental change can be examined. At pre-Alpine Lake Mondsee in Austria, a range of proxies, including pollen, stable isotope geochemistry and elemental data from μXRF scanning, were used to establish the nature and timing of response to rapid environmental changes between 10 and 15 cal ka BP (Lauterbach et al. 2011). A combination of varve counting and the oxygen isotope record from ostracods was used to tie the Mondsee sequence to the GICC05 chronology from the NGRIP ice core (Rasmussen et al. 2006). XRF data clearly indicate the stratigraphic changes associated with the Younger Dryas, with increased values of Mg and reduced Ca (Fig. 7.7). However, detailed comparison of proxies indicates variability in the timing of the response to cooling at the onset of the Younger Dryas (Greenland Stadial-1). A shift in $\delta^{18}O$ values indicates declining temperature and is associated with an increase in non-arboreal pollen. The sedimentary response however, is somewhat slower. Ca (reflecting reduced authigenic precipitation of calcite in a colder lake) does not start to decline for another c. 125 years. Increased detrital inputs from surrounding dolomite, represented by the Mg profile, gradually increase at the same time as Ca declines, with a rapid influx occurring c. 12.4 cal ka BP. This record indicates a lag in the detrital response to Younger Dryas cooling of some 150–300 years. Lauterbach et al. (2011) also note a more rapid response of proxies to Holocene warming than to the increased temperatures at the onset of the Lateglacial Interstadial.

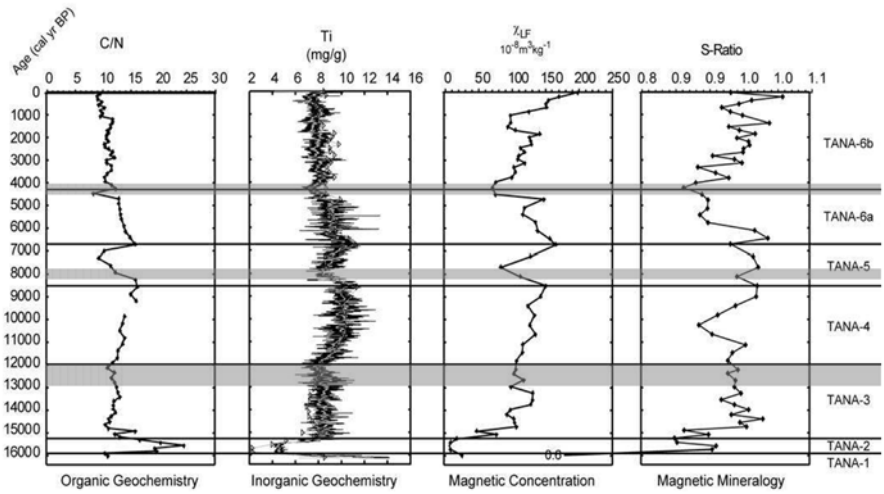

Fig. 7.8 Comparison of XRF scanning data with magnetic properties and bulk organic geochemistry from Lake Tana, Ethiopia. XRF data were converted to mg/kg by regression of scanning data against conventional XRF analyses of dry sediment. *Grey bars* designate the timing of drought episodes identified in the record. (Adapted from Marshall et al. (2011))

Marshall et al. (2011) used a 17,000 year sequence from Lake Tana in northern Ethiopia, the source of the Blue Nile, to develop a record of hydrological variability. μXRF data confirmed previous palaeoecological investigations (Lamb et al. 2007) that low lake levels, characterised by high Ca, coincided with Heinrich Event 1. The lake became overflowing at 15.3 cal ka BP, with Ca and Sr declining rapidly and then maintaining low values throughout the remainder of the record. After this, the Ti record, supported by mineral magnetic data, is used to infer changing hydrological conditions, with reduced detrital inputs indicating drier episodes (Fig. 7.8). Reduced run-off is observed between 13.0 and 12.5 cal ka BP, possibly corresponding to the onset of the Younger Dryas. Lower values of Ti are recorded around 8 and 4.2 cal ka BP, accompanied by lower magnetic susceptibility values and a reduction in the S-ratio of the magnetic mineralogy. Marshall et al. (2011) argue that during dry phases, magnetic grain-size decreases and formation of anti-ferrimagnetic minerals (e.g., haematite) occurs, which is then washed into the lake at the culmination of the drought episode. The fluctuations in the Ti record are relatively subtle, but inferred droughts also coincide with seismic reflectors. It appears that the overflowing conditions of Lake Tana make it a less sensitive recorder of abrupt changes in moisture availability during the Holocene, but a combination of geochemical and mineral magnetic analysis provides evidence of drought events. The 4.2 ka event is thought to have contributed to the collapse of the Egyptian Old Kingdom (Bell 1971) and the geochemical and magnetic evidence from Lake Tana indicates that there were reduced flows from the source of the Nile at this time (Marshall et al. 2011).

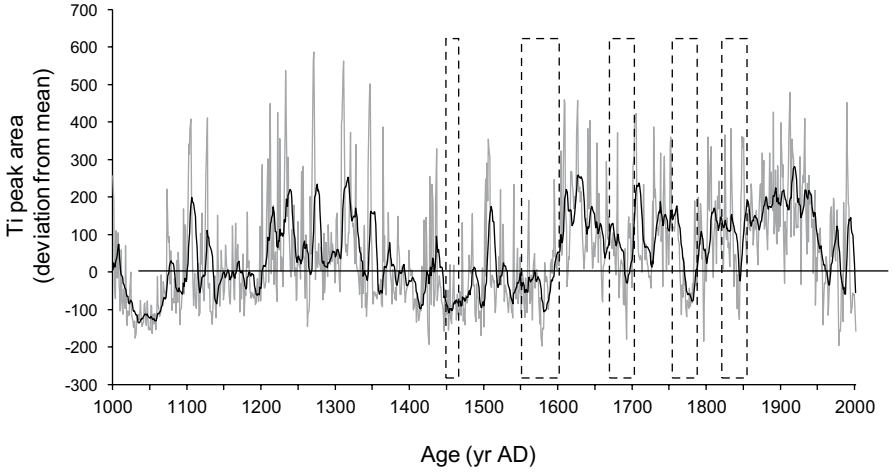

Fig. 7.9 Ti record from Laguna de Juanacatlán, Mexico, presented as deviation from the mean, compared with known historical drought episodes in Mexico—AD. (Adapted from Metcalfe et al. (2010))

At Laguna de Juanacatlán in west-central Mexico, Metcalfe et al. (2010) established that the Ti record is a reliable record of catchment run-off over the last 2000 years in this basin. Laminated sediments are composed of diatom-rich organic layers and pink clay layers, the Ti profile closely tracking the pink layers. Ti values from μXRF scanning were compared with conventional XRF measurements through the core and confirmed the trends evident from the scanning data. Sediment trap data confirmed clay layers are deposited during the summer wet season. A robust age model developed from 26 radiocarbon dates on the full 7 m sequence spanning c. 6000 years enabled comparison of the recent sediments with historical droughts. Lower Ti values (expressed as deviation from the mean) occurred during several time periods within the last 500 years (Fig. 7.9), which have been identified as dry intervals from Spanish Colonial documentary sources. Nearby meteorological records only cover the period 1961–1991 and are incomplete during the 1980s, so the comparison with historical records is a useful alternative means of checking the validity of the Ti interpretation.

Varve chronologies from two crater lakes in the Valle de Santiago, central Mexico show a more complex relationship with Ti (Kienel et al. 2009), demonstrating the importance of understanding local catchment characteristics and how they are influenced by climate. The varved sediments are characterised by high Ca values in carbonate layers deposited during the winter, whereas Ti is deposited in the lakes from both run off in the wet season (summer) and aeolian sources during the dry season (winter). Kienel et al. (2009) propose that drought episodes could be identified when Ti and Ca are negatively correlated. This is interpreted as indicating that sub-laminae are more clearly separated, with enhanced winter evaporation and rainfall restricted to summer. Unfortunately, this hypothesis cannot be tested as

the lakes are now dry, but the periods of drought identified from the geochemical data correspond reasonably well to known historical droughts and suggest a link to ENSO.

Records of Human Activity

Although most palaeolimnological studies using XRF scanning have focused on climatic reconstructions, the technique can also provide insights into past human activity. An increase in detrital elements may be the result of anthropogenic disturbance of catchment slopes. For example, Arnaud et al. (2012) presented evidence for soil destabilisation and changes in erosion patterns after 4.4 cal ka BP at Lake Bourget in the French Alps, although they argued that the dominant control throughout their record is climatic rather than anthropogenic. At Lake Paladru to the southwest of Lake Bourget, Simonneau et al. (2013) observed an increase in Ti from very low background levels at around 2.7 cal ka BP, which they interpreted as a response to more intense exploitation of the surrounding catchment during the Iron Age, with deeper ploughing of soils. Increased detrital inputs since then, particularly during the last 1600 years appear to have led to elevated nutrient levels and greater algal productivity, according to quantitative organic petrography (Simonneau et al. 2013).

In addition to evidence of catchment disturbance and soil erosion, XRF data can be used to identify pollution resulting from historic and pre-historic mining activity. Guyard et al. (2007) analysed sediment cores from Lake Bramant in the western Alps spanning the last c. 4 cal ka BP. A distinct peak in copper was identified (presented as Cu/Rb) and related to Bronze Age mining c. 3.87–3.77 cal ka BP (Fig. 7.10). Further up the core, another Cu peak is associated with a dramatic increase in Pb values, corresponding to the peak intensity of lead mining activity during the Roman period. It is, however, possible that the reduced levels for Rb between 430 and 455 cm and below 480 cm exaggerate the Cu/Rb peaks in the Bronze Age. In this case, it would have been beneficial to obtain some conventional XRF data based on dry mass concentrations, which could be used to calibrate the scanning data and provide a quantitative reconstruction of element concentrations. A more recent study of pollution in Lake Windermere, UK, combining μXRF scanning with WD-XRF data and stable Pb isotope measurements reveals a complex pattern of change over the last 500 years (Miller et al. 2014), with a notable increase in Pb, Zn and Cu since the 1930s. These elevated concentrations of Pb in the upper sediments are attributed to a combination of pollution from mining activity, coal burning and gasoline combustion along with a naturally derived component from the catchment. The lag between periods of mining and Pb entering the system is attributed to trapping of sediment in lakes upstream (Miller et al. 2014).

The first sedimentary record of Colonial copper smelting pollution in Mexico was obtained from Lago de Zirahuen, by Davies et al. (2004) where elevated levels of Cu and Pb were revealed using atomic absorption spectrometry. The period of

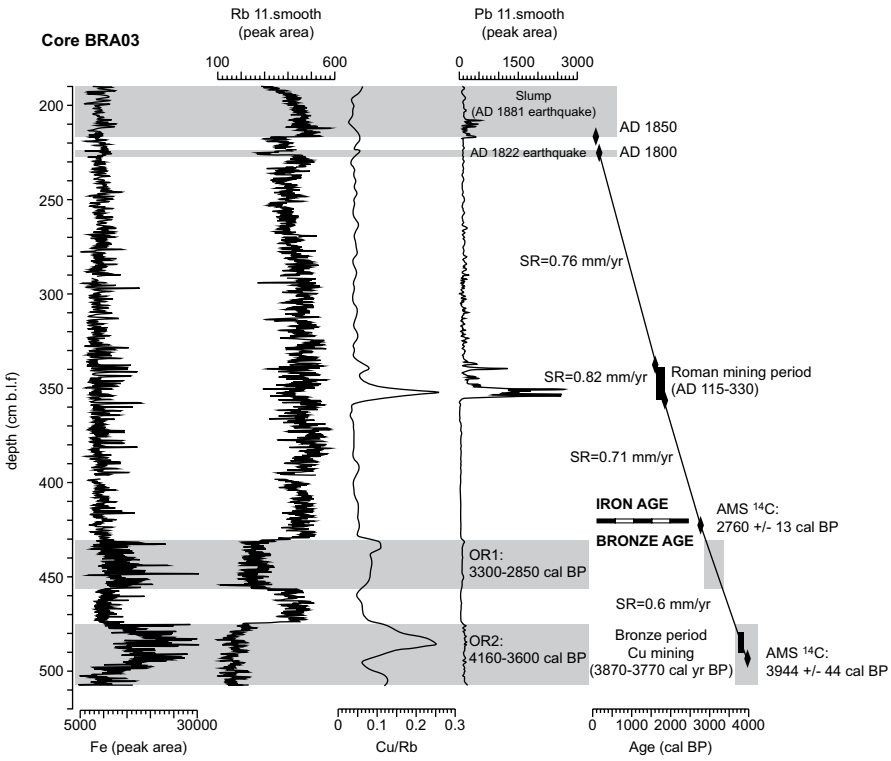

Fig. 7.10 µXRF data from Lake Bramant, French Alps, reveal evidence of prehistoric mining activity in the catchment from Cu/Rb and Pb values. The age model is based on two radiocarbon dates and varve counting. (From Guyard et al. (2007), with permission from Elsevier)

smelting activity is bracketed between tephra layers from two historical volcanic eruptions—Jorullo (AD 1759–1764) and Paricutín (AD 1943–1952), with maximum values of Cu in the 10 cm above the Jorullo tephra. The site was re-cored and XRF scans reveal results consistent with the previous study (Fig. 7.11). In the new record from Lago de Zirahuen, Cu peak area values are low, with maximum values during the period of smelting of c. 100. This demonstrates that even at relatively low values, µXRF scanning can provide reliable signals. It is interesting to note that an increase in Pb values is not observed in the µXRF scanning data, but elevated values of c. 15 mg/kg (compared with background levels of c. 10 mg/kg) were observed in the original study.

To date, there have been relatively few palaeolimnological studies which have used XRF scanning to explore pollution records (Guyard et al. 2007; Miller et al. 2014). There is considerable potential, both as a tool for examining historical and pre-historic anthropogenic impacts, but also as a tool for identifying recent environmental disturbances.

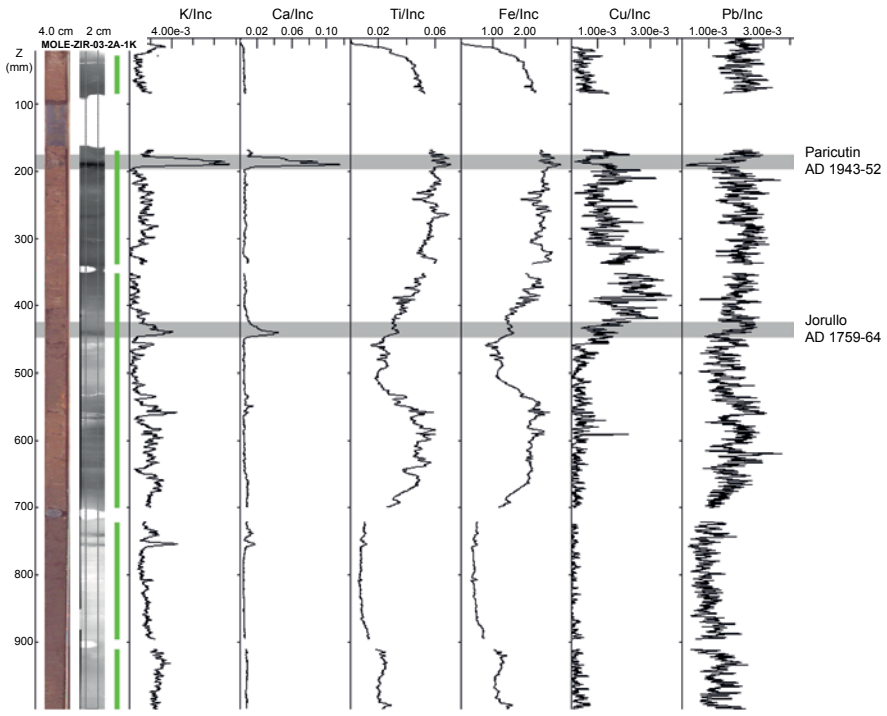

Fig. 7.11 μXRF data from the Zirahuen Basin, Mexico spanning the last c. 1000 years. Fe and Ti represent detrital inputs, K and Ca highlight the tephra layers. Cu and Pb are potential indicators of pollution from Colonial copper smelting, which reached its peak in the basin during the late eighteenth century. The highest Cu values are bracketed by tephras from Volcan Jorullo (AD 1759–1764) and Volcan Paricutin (AD 1943) (Davies et al. unpubl. data)

Summary and Conclusions

Within the last decade, micro-XRF scanning has become an increasingly powerful tool in palaeolimnology. As part of a suite of initial core analyses, elemental data provide rapid assessment of key stratigraphic changes creating a framework for a more targeted approach for the processing of more time-consuming proxy analyses. Rapid characterisation of sediments in unprecedented detail has also led to innovative developments, such as in varve counting. Significant advances have been made in the development of continuous, high-resolution palaeoclimatic records worldwide, with XRF scanning making a major contribution to the insights obtained from large lake drilling projects. Elemental data from XRF scanning have enabled the identification of rapid, abrupt climatic changes and thrown light on the relationships between proxies and the leads and lags in responses of different components of the lake-catchment system. A growing area is the use of μXRF scanning to identify event deposits (e.g., flooding, seismic events, volcanic eruptions). Rapid

assessment of the recurrence interval and magnitude of such events can contribute valuable data for agencies involved in planning for such hazards.

With a proliferation of data that is relatively easy to generate, some caution needs to be applied in order to ensure that results are robust. A key question at the start of any study should be—are fully quantitative data required? If so, then recommendations by Boyle et al., this volume should be followed in order to produce reliable concentration data for elements of interest. Checks should be made as to whether organic and/or water content are having an effect on downcore element profiles. It is important to ensure that environmental interpretations are grounded in knowledge about local catchment and in-lake processes as well as regional scale factors which may be the broader focus of the investigation. Interpretations from one lake basin should not be assumed to translate to another. We recommend that a clear relationship should be established between present day environmental processes and elemental concentrations in the sediment wherever possible. This can be achieved for example, through deployment of sediment traps, elemental and mineralogical analysis of the surrounding catchment soils and rocks and limnological monitoring. Where sampling the modern environment is not possible, or there is a 'no-analogue' situation, it is preferable that a multi-proxy approach is adopted to underpin interpretations from μXRF scanning data. These recommendations are standard for many aspects of palaeolimnology, but given the range of processes which may lead to elemental variations, they are of particular relevance for μXRF scanning studies.

A key theme arising from this review is the non-stationary behaviour of lake systems. This may manifest itself in various ways. The decoupling of the XRF data from climate reported by Arnaud et al. (2012) in their Holocene Alpine lake record occurred when lake level rose and altered basin morphology. Kylander et al. (2011) identified changes in the relationships between elements in different stratigraphic units over their 46 cal ka BP record from Les Echets. It is important to consider the possibility that the environmental interpretation of an element or ratio may not be constant through time as lake basins respond to environmental changes. Developing correlation matrices to identify changes in relationships between elements with lithology helps to highlight issues of non-stationarity.

To date, much of the focus of μXRF scanning in lake sediments has been on the environmental interpretation of detrital components (source, transport mechanism, rates of supply, extreme events, weathering processes). Forty-nine element integrals and ratios have been used in the palaeolimnological literature from core scanner data. Ti is the most widely used element and has been used both as an indicator of changing allochthonous inputs which may be linked to a variety of climatic drivers or sources and secondly as a normalising tool to allow determination of the role of within-lake processes such as redox conditions, lake stratification or authigenic carbonate precipitation. The use of Ca/Ti or Ca has also become an important tool for reconstructing hydrological variability, particular in closed basin lakes which are particularly sensitive to lake level change. The main focus of studies to date has been on the stratigraphic pattern of changing elemental abundances, so few authors have made the extra step to calibrating the XRF data to give absolute values equivalent to dry mass concentrations. Improving the quality of reconstructions through calibration should be a priority for future studies.

There is considerable potential for further development of the μXRF scanning in palaeolimnology, including:

- the examination of internal lake processes, such as changing redox conditions and nutrient status, through analysis of Fe, Mn, S and P profiles. To date, relatively few studies focus on these elements and interpretation can be complex.
- a detailed assessment of the potential for the use of Br in combination with possibly Cl and/or I (where measureable) as a proxy for coastal storm activity. Although Br is related to organic matter, in maritime settings, excess of these elements above background levels could indicate increased sea spray.
- the investigation of pollution histories and as a tool for rapid assessment of environmental impacts.
- further experimental work on the geochemical signatures of different types of tephra in a range of background sediment chemistries.

Due to the highly variable nature of lake sediments and the diverse range of internal and external mechanisms affecting their geochemical composition, interpretation of μXRF scanning data is not always straightforward. The potential for non-stationarity must be a key consideration for all studies. However, this review has demonstrated the valuable insights into environmental change and processes over a range of timescales, both natural and anthropogenic that can be obtained through the application of μXRF core scanning.

References

Arnaud F, Révillon S, Debret M, Revel M, Chapron E, Jacob J, Giguet-Covex C, Poulenard J, Magny M (2012) Lake Bourget regional erosion patterns reconstruction reveals Holocene NW European Alps soil evolution and paleohydrology. Quat Sci Rev 51:81–92. doi:10.1016/j.quascirev.2012.07.025

Aufgebauer A, Panagiatopoulos K, Wagner B, Schaebitz F, Viehberg FA, Vogel H, Zanchetta G, Sulpizio R, Leng MJ, Damaschke M (2012) Climate and environmental change over the last 17 ka recorded in sediments from Lake Prespa (Albania/F.Y.R. of Macedonia/Greece). Quat Int 274:122–135. doi:10.1016/jquaint.2012.02.015

Bakke J, Lie Ø, Heegaard E, Dokken T, Haug G, Birks H, Dulski P, Nilsen T (2009) Rapid oceanic and atmospheric changes during the Younger Dryas cold period. Nat Geosci 2:202–205. doi:10.1038/ngeo439

Balascio N, Zhang Z, Bradley R, Perren B, Dahl S, Bakke J (2011) A multi-proxy approach to assessing isolation basin stratigraphy from the Lofoten Islands, Norway. Quat Res 75:288–300. doi:10.1016/j.yqres.2010.08.012

Bell B (1971) The dark ages in ancient history: the first dark age in Egypt. Am J Archaeol 75:1–25

Berntsson A, Rosqvist GC, Velle G (2014) Late-Holocene temperature and precipitation changes in Vindelfjällen, mid-western Swedish Lapland, inferred from chironomid and geochemical data. Holocene 24:78–92. doi:10.1177/0959683613512167

Boës X, Rydberg J, Martinez-Cortizas A, Bindler R, Renberg I (2011) Evaluation of conservative lithogenic elements (Ti, Zr, Al, and Rb) to study anthropogenic element enrichments in lake sediments. J Paleolimnol 46:75–87

Boyle JF (2001) Inorganic geochemical methods in palaeolimnology. In Last WM, Smol JP (eds) Tracking environmental change using lake sediments: physical and geochemical methods, vol 2. Kluwer, Dordrecht, pp 83–141

Bronk Ramsey C, Staff R, Bryant C, Brock F, Kitagawa H, Plicht J, Schlolaut G, Marshall M, Brauer A, Lamb H, Payne R, Tarasov P, Haraguchi T, Gotanda K, Yonenobu H, Yokoyama Y, Tada R, Nakagawa T (2012) A complete terrestrial radiocarbon record for 11.2–52.8 kyr B.P. Science 338:370–374. doi:10.1126/science.1226660

Brown E (2011) Lake Malawi's response to "megadrought" terminations: sedimentary records of flooding, weathering and erosion. Palaeogeogr Palaeoclimatol Palaeoecol 303:120–125. doi:10.1016/j.palaeo.2010.01.038

Brown E, Johnson T, Scholz C, Cohen A, King J (2007) Abrupt change in tropical African climate linked to the bipolar seesaw over the past 55,000 years. Geophys Res Lett doi:10.1029/2007GL031240

Burn M, Palmer S (2014) Solar forcing of Caribbean drought events during the last millennium. J Quat Sci 29:827–836. doi:10.1002/jqs.2660

Burnett A, Soreghan M, Scholz C, Brown E (2011) Tropical East African climate change and its relation to global climate: a record from Lake Tanganyika, tropical East Africa, over the past 90 + kyr. Palaeogeogr Palaeoclimatol Palaeoecol 303:155–167. doi:10.1016/j.palaeo.2010.02.011

Chawchai S, Chabangborn A, Kylander M, Löwemark L, Mörth C, Blaauw M, Klubseang W, Reimer P, Fritz S, Wohlfarth B (2013) Lake Kumphawapi—an archive of Holocene palaeoenvironmental and palaeoclimatic changes in northeast Thailand. Quat Sci Rev 68:59–75. doi:10.1016/j.quascirev.2013.01.030

Clift P, Wan S, Blusztajn J (2014) Reconstructing chemical weathering, physical erosion and monsoon intensity since 25 Ma in the northern South China Sea: a review of competing proxies. Earth Sci Rev 130:86–102. doi:10.1016/j.earscirev.2014.01.002

Cohen AS (2003) Paleolimnology: the history and evolution of lake systems. Oxford University Press, New York, p 528

Corella J, Brauer A, Mangili C, Rull V, Vegas-Vilarrúbia T, Morellón M, Valero-Garcés B (2012) The 1.5-ka varved record of Lake Montcortès (southern Pyrenees, NE Spain). Quat Res 78:323–332. doi:10.1016/j.yqres.2012.06.002

Croudace IW, Rindby A, Rothwell RG (2006) ITRAX: description and evaluation of a new multi-function X-ray core scanner. In: Rothwell RG (ed) New techniques in sediment core analysis, vol 267. Geological Society Special Publication, pp 51–63

Cuven S, Francus P, Lamoureux S (2010) Estimation of grain-size variability with micro X-ray fluorescence in laminated lacustrine sediments, cape bounty, Canadian High Arctic. J Paleolimnol 44:803–817. doi:10.1007/s10933-010-9453-1

Cuven S, Francus P, Lamoureux S (2011) Mid to Late Holocene hydroclimatic and geochemical records from the varved sediments of East lake, Cape Bounty, Canadian High Arctic. Quat Sci Rev 30:2651–2665. doi:10.1016/j.quascirev.2011.05.019

Czymzik M, Brauer A, Dulski P, Plessen B, Naumann R, Grafenstein U, Scheffler R (2013) Orbital and solar forcing of shifts in mid- to late Holocene flood intensity from varved sediments of pre-alpine Lake Ammersee (southern Germany). Quat Sci Rev 61:96–110. doi:10.1016/j.quascirev.2012.11.010

Damaschke M, Sulpizio R, Zanchetta G, Wagner B, Böhm A, Nowaczyk N, Rethemeyer J, Hilgers A (2013) Tephrostratigraphic studies on a sediment core from Lake Prespa in the Balkans. Clim Past 9:267–287. doi:10.5194/cp-9-267-2013

Davies SJ, Metcalfe SE, MacKenzie AB, Newton AJ, Endfield GH, Farmer JG (2004) Environmental changes in the Zirahuén basin, Michoacán, Mexico, during the last 1000 years. J Paleolimnol 31:77–98. doi:10.1023/B:JOPL.0000013284.21726.3d

Davies, SJ, Israde, I, Lozano, S, Ortega, B (unpubl.)

Davison W (1993) Iron and manganese in lakes. Earth Sci Rev 34:119–163

De Boer EJ, Tjallingii R, Velez MI, Rijsdijk KF, Vlug A, Reichart GJ, Prendergast AL, de Louw PGB, Florens FBV, Baider C, Hooghiemstra H (2014) Climate variability in the SW Indian ocean from an 8000-yr multi-proxy record in the Mauritian lowlands shows a middle

to late Holocene shift from negative IOD-state to ENSO-state. Quat Sci Rev 86:175–189. doi:10.1016/j.quascirev.2013.12.026

Elbert J, Grosjean M, Gunten L, Urrutia R, Fischer D, Wartenburger R, Ariztegui D, Fujak M, Hamann Y (2012) Quantitative high-resolution winter (JJA) precipitation reconstruction from varved sediments of Lago Plomo 47°S, Patagonian Andes, AD 1530–2002. Holocene 22:465–474. doi:10.1177/0959683611425547

Elbert E, Wartenburger R, von Gunten L, Urrutia R, Fischer D, Fujak M, Hamann Y, Greben ND, Grosjean M (2013) Late Holocene air temperature reconstructed from sediments of Laguna Escondida, Patagonia, Chile (45°S 30'W). Palaeogeogr Palaeoclimatol Palaeoecol 369:482–492. doi:10.1016/j.palaeo.2012.11.013

Engstrom DR, Wright HE Jr (1984) Chemical stratigraphy of lake sediments as a record of environmental change. In: Haworth EY, Lund JWG (eds) Lake sediments and environmental history. Leicester University Press, Leicester, pp 11–68

Eugster HP, Hardie LA (1978) Saline lakes. In: Lerman A (ed) Lakes: chemistry, geology, physics. Springer, New York, pp 237–289

Fedotov A, Phedorin M, Enushchenko I, Vershinin K, Melgunov M, Khodzher T (2012) A reconstruction of the thawing of the permafrost during the last 170 years on the Taimyr Peninsula (East Siberia, Russia). Glob Planet Change 98–99:139–152. doi:10.1016/j.gloplacha.2012.09.002

Fernandez M, Björck S, Wohlfarth B, Maidana N, Unkel I, Van der Putten N (2013) Diatom assemblage changes in lacustrine sediments from Isla de los Estados, southernmost South America, in response to shifts in the southwesterly wind belt during the last deglaciation. J Paleolimnol 50:433–446. doi:10.1007/s10933-013-9736-4

Foerster V, Junginger A, Langkamp O, Gebru T, Asrat A, Umer M, Lamb H, Wennrich V, Rethemeyer J, Nowaczyk N, Trauth M, Schaebitz F (2012) Climatic change recorded in the sediments of the Chew Bahir basin, southern Ethiopia, during the last 45,000 years. Quat Int 274:25–37. doi:10.1016/j.quaint.2012.06.028

Francus P, Lamb H, Nakagawa T, Marshall M, Brown E, Suigetsu 2006 project members (2009) The potential of high-resolution X-ray fluorescence core scanning: applications in paleolimnology. PAGES News 17:93–95

Gilfedder BS, Petri M, Wessels M, Biester H (2011) Bromine species fluxes from Lake Constance's catchment and a preliminary lake mass balance. Geochim et Cosmochim Acta 75:3385–3401. doi:10.1016/j.gca.2011.03.021

Guyard H, Chapron E, St-Onge G, Anselmetti F, Arnaud F, Magand O, Francus P, Mélières M-A (2007) High-altitude varve records of abrupt environmental changes and mining activity over the last 4000 years in the Western French Alps (Lake Bramant, Grandes Rousses Massif). Quat Sci Rev 26:2644–2660. doi:10.1016/j.quascirev.2007.07.007

Haberzettl T, Fey M, Lücke A, Maidana N, Mayr C, Ohlendorf C, Schäbitz F, Schleser G, Wille M, Zolitschka B (2005) Climatically induced lake level changes during the last two millennia as reflected in sediments of Laguna Potrok Aike, southern Patagonia (Santa Cruz, Argentina). J Paleolimnol 33:283–302. doi:10.1007/s10933-004-5331-z

Haberzettl T, Corbella H, Fey M, Janssen S, Lucke A, Mayr C, Ohlendorf C, Schabitz F, Schleser G, Wille M, Wulf S, Zolitschka B (2007) Lateglacial and Holocene wet–dry cycles in southern patagonia: chronology, sedimentology and geochemistry of a lacustrine record from Laguna Potrok Aike, Argentina. Holocene 17:297–310. doi:10.1177/0959683607076437

Haberzettl T, Anselmetti F, Bowen S, Fey M, Mayr C, Zolitschka B, Ariztegui D, Mauz B, Ohlendorf C, Kastner S, Lücke A, Schäbitz F, Wille M (2009) Late Pleistocene dust deposition in the Patagonian steppe—extending and refining the paleoenvironmental and tephrochronological record from Laguna Potrok Aike back to 55 ka. Quat Sci Rev 28:2927–2939. doi:10.1016/j.quascirev.2009.07.021

Hodell D, Turchyn A, Wiseman C, Escobar J, Curtis J, Brenner M, Gilli A, Mueller A, Anselmetti F, Ariztegui D, Brown E (2012) Late glacial temperature and precipitation changes in the lowland Neotropics by tandem measurement of $\delta^{18}O$ in biogenic carbonate and gypsum hydration water. Geochim et Cosmochim Acta 77:352–368. doi:10.1016/j.gca.2011.11.026

Jones A, Lewin J, Macklin M (2010) Flood series data for the later Holocene: available approaches, potential and limitations from UK alluvial sediments. Holocene 20:1123–1135. doi:10.1177/0959683610369501

Jouve G, Francus P, Lamoureux S, Provencher-Nolet L, Hahn A, Haberzettl T, Fortin D, Nuttin L, The PASADO Science Team (2013) Microsedimentological characterization using image analysis and μ-XRF as indicators of sedimentary processes and climate changes during Lateglacial at Laguna Potrok Aike, Santa Cruz, Argentina. Quat Sci Rev 71:191–204. doi:10.1016/j.quascirev.2012.06.003

Kalugin I, Daryin A, Smolyaninova L, Andreev A, Diekmann B, Khlystov O (2007) 800-yr-long records of annual air temperature and precipitation over southern Siberia inferred from Teletskoye Lake sediments. Quat Res 67:400–410. doi:10.1016/j.yqres.2007.01.007

Kalugin I, Darin A, Rogozin D, Tretyakov G (2013) Seasonal and centennial cycles of carbonate mineralisation during the past 2500 years from varved sediment in Lake Shira, South Siberia. Quat Int 290–291:245–252. doi:10.1016/j.quaint.2012.09.016

Kämpf L, Brauer A, Dulski P, Lami A, Marchetto A, Gerli S, Ambrosetti W, Guilizzoni P (2012) Detrital layers marking flood events in recent sediments of Lago Maggiore (N. Italy) and their comparison with instrumental data. Freshw Biol 57:2076–2090. doi:10.1111/j.1365-2427.2012.02796.x

Kienel U, Bowen S, Byrne R, Park J, Böhnel H, Dulski P, Luhr J, Siebert L, Haug G, Negendank J (2009) First lacustrine varve chronologies from Mexico: impact of droughts, ENSO and human activity since AD 1840 as recorded in maar sediments from Valle de Santiago. J Paleolimnol 42:587–609. doi:10.1007/s10933-009-9307-x

Kylander M, Ampel L, Wohlfarth B, Veres D (2011) High-resolution X-ray fluorescence core scanning analysis of Les Echets (France) sedimentary sequence: new insights from chemical proxies. J Quat Sci 26:109–117. doi:10.1002/jqs.1438

Kylander M, Lind E, Wastegard S, Lowemark L (2012) Recommendations for using XRF core scanning as a tool in tephrochronology. Holocene 22:371–375. doi:10.1177/0959683611423688

Lamb H, Bates C, Coombes P, Marshall M, Umer M, Davies S, Dejen E (2007) Late Pleistocene desiccation of Lake Tana, source of the Blue Nile. Quat Sci Rev 26:287–299. doi:10.1016/j.quascirev.2006.11.020

Lane C, Chorn B, Johnson T (2013) Ash from the Toba supereruption in Lake Malawi shows no volcanic winter in East Africa at 75 ka. Proc Natl Acad Sci U S A 110:8025–8029. doi:10.1073/pnas.1301474110

Lauterbach S, Brauer A, Andersen N, Danielopol D, Dulski P, Hüls M, Milecka K, Namiotko T, Obremska M, Grafenstein U, Participants D (2011) Environmental responses to Lateglacial climatic fluctuations recorded in the sediments of pre-alpine Lake Mondsee (northeastern Alps). J Quat Sci 26:253–267. doi:10.1002/jqs.1448

Litt T, Krastel S, Sturm M, Kipfer R, Örcen S, Heumann G, Franz S, Ülgen U, Niessen F (2009) "PALEOVAN", International continental scientific drilling program (ICDP): site survey results and perspectives. Quat Sci Rev 28:1555–1567. doi:10.1016/j.quascirev.2009.03.002

Löwemark L, Chen H, Yang T, Kylander M, Yu E, Hsu Y, Lee T, Song S, Jarvis S (2011) Normalizing XRF-scanner data: A cautionary note on the interpretation of high-resolution records from organic-rich lakes. J Asian Earth Sci 40:1250–1256. doi:10.1016/j.jseaes.2010.06.002

Mackareth FGH (1966) Some chemical observations on post-glacial lake sediments. Philos Trans R Soci Lond B 250:165–213

Marshall MH, Lamb HF, Huws D, Davies SJ, Bates CR, Bloemendahl J, Boyle JF, Leng MJ, Umer M, Bryant CL (2011). Late Pleistocene and Holocene drought events at Lake Tana, the source of the Blue Nile. Glob Planet Change 78:147–161. doi:10.1016/j.glopacha.2011.06.004

Marshall M, Schlolaut G, Nakagawa T, Lamb H, Brauer A, Staff R, Ramsey C, Tarasov P, Gotanda K, Haraguchi T, Yokoyama Y, Yonenobu H, Tada R (2012) A novel approach to varve counting using μXRF and X-radiography in combination with thin-section microscopy, applied to the Late Glacial chronology from Lake Suigetsu, Japan. Quat Geochronol 13:70–80. doi:10.1016/j.quageo.2012.06.002

Martin-Puertas C, Valero-Garcés B, Mata MP, Moreno A, Giralt S, Martinez-Ruiz F, Jimenéz-Espejo F (2011) Geochemical processes in a Mediterranean lake: a high-resolution study of the last 4,000 years in Zoñar Lake, southern Spain. J Paleolimnol 46:405–421. doi:10.1007/s10933-009-9373-0

Martin-Puertas C, Brauer A, Dulski P, Brademann B (2012) Testing climate–proxy stationarity throughout the Holocene: an example from the varved sediments of Lake Meerfelder Maar (Germany). Quat Sci Rev 58:56–65. doi:10.1016/j.quascirev.2012.10.023

Melles M, Brigham-Grette J, Minyuk PS, Nowaczyk NR, Wennrich V, Andreev AA, Coletti A, Cook TL, Haltia-Hovi E, Kukkonen M, Lohzkin AV, Rosén P, Tarasov P, Vogel H, Wagner B (2012) 2.8 million years of Arctic climate change from Lake El'gygytgyn, NE Russia. Science 337:315–320. doi:10.1126/science.1222135

Metcalfe SE, Jones MD, Davies SJ, Noren A, MacKenzie A (2010) Climate variability over the last two millennia in the North American Monsoon region, recorded in laminated lake sediments from Laguna de Juanacatlan, Mexico. Holocene 20:1195–1206. doi:10.1177/0959683610371994

Miller H, Croudace IW, Bull JM, Cotterill CJ, Dix JK, Taylor RN (2014) Sediment lake record of anthropogenic and natural inputs to Windermere (English Lake District) using double-spike lead isotopes, radiochronology, and sediment microanalysis. Environ Sci Technol 48:7254–7263. doi:10.1021/es5008998

Moreno A, Giralt S, Valero-Garcés B, Sáez A, Bao R, Prego R, Pueyo J, González-Sampériz P, Taberner C (2007) A 14kyr record of the tropical Andes: the Lago Chungará sequence (18°S, northern Chilean Altiplano). Quat Int 161:4–21. doi:10.1016/j.quaint.2006.10.020

Moreno A, Valero-Garcés B, González-Sampériz P, Rico M (2008) Flood response to rainfall variability during the last 2000 years inferred from the Taravilla lake record (Central Iberian Range, Spain). J Paleolimnol 40:943–961. doi:10.1007/s10933-008-9209-3

Moreno A, Lopéz-Merino L, Leira M, Marco-Barba M, González-Sampériz P, Valero-Garcés BL, Lopéz-Saez J, Santos L, Mata P, Ito E (2011) Revealing the last 13,500 years of environmental history from the multi-proxy record of a mountain lake (Lago Enol, northern Iberian Peninsula). J Paleolimnol 46:327–349. doi:10.1007/s10933-009-9387-7

Mueller A, Islebe G, Hillesheim M, Grzesik D, Anselmetti F, Ariztegui D, Brenner M, Curtis J, Hodell D, Venz K (2009) Climate drying and associated forest decline in the lowlands of northern Guatemala during the Late Holocene. Quat Res 71:133–141. doi:10.1016/j.yqres.2008.10.002

Nakagawa T, Gotanda K, Haraguchi T, Danhara T, Yonenobu H, Brauer A, Yokoyama Y, Tada R, Takemura K, Staff R, Payne R, Ramsey C, Bryant C, Brock F, Schlolaut G, Marshall M, Tarasov P, Lamb H (2012) SG06, a fully continuous and varved sediment core from Lake Suigetsu, Japan: stratigraphy and potential for improving the radiocarbon calibration model and understanding of late Quaternary climate changes. Quat Sci Rev 36:164–176. doi:10.1016/j.quascirev.2010.12.013

Neugebauer I, Brauer A, Dräger N, Dulski P, Wulf S, Plessen B, Mingram J, Herzschuh U, Brande A (2012) A younger dryas varve chronology from the Rehwiese palaeolake record in NE-Germany. Quat Sci Rev 36:91–102. doi:10.1016/j.quascirev.2011.12.010

Niemann H, Matthias I, Michalzik B, Behling H (2013) Late Holocene human impact and environmental change inferred from a multi-proxy lake sediment record in the Loja region, southeastern Ecuador. Quat Int 308/309:253–264. doi:10.1016/j.quaint.2013.03.017

Nuttin L, Francus P, Preda M, Ghaleb B, Hillaire-Marcel C, The PASADO Science Team (2013) Authigenic, detrital and diagenetic minerals in the Laguna Potrok Aike sediment sequence. Quat Sci Rev 71:109–118. doi:10.1016/j.quatscirev.2012.09.027

Olsen J, Anderson N, Leng M (2013) Limnological controls on stable isotope records of late-Holocene palaeoenvironment change in SW Greenland: a paired lake study. Quat Sci Rev 66:85–95. doi:10.1016/j.quascirev.2012.10.043

Rasmussen S, Andersen K, Svensson A, Steffensen J, Vinther B, Clausen H, Siggaard-Andersen M, Johnsen S, Larsen L, Dahl-Jensen D, Bigler M, Röthlisberger R, Fischer H, Goto-Azuma K, Hansson M, Ruth U (2006) A new Greenland ice core chronology for the last glacial termination. J Geophys Res. doi:10.1029/2005JD006079

Richter TO, Van der Gaast S, Koster B, Vaars A, Gieles R, de Stigter HC, de Haas H, van Weering TCE (2006) The Avaatech XRF core scanner: technical description and applications to NE Atlantic sediments. In: Rothwell RG (ed) New techniques in sediment core analysis, vol 267. Geological Society Special Publication, pp 39–50. doi:10.1144/GSL.SP.2006.267.01.03

Schillereff D, Chiverrell R, Macdonald N, Hooke J (2014) Flood stratigraphies in lake sediments: a review. Earth Sci Rev 135:17–37. doi:10.1016/j.earscirev.2014.03.011

Schlolaut G, Marshall M, Brauer A, Nakagawa T, Lamb H, Staff R, Ramsey C, Bryant C, Brock F, Kossler A, Tarasov P, Yokoyama Y, Tada R, Haraguchi T (2012) An automated method for varve interpolation and its application to the late glacial chronology from Lake Suigetsu, Japan. Quat Geochronol 13:52–69. doi:10.1016/j.quageo.2012.07.005

Schlolaut G, Brauer A, Marshall M, Nakagawa T, Staff R, Ramsey C, Lamb H, Bryant C, Naumann R, Dulski P, Brock F, Yokoyama Y, Tada R, Haraguchi T, Suigetsu 2006 project members (2014) Event layers in the Japanese Lake Suigetsu "SG06" sediment core: description, interpretation and climatic implications. Quat Sci Rev 83:157–170. doi:10.1016/j.quascirev.2013.10.026

Schnurrenberger D, Kelts K, Johnson T, Shane L, Ito E (2001) National lacustrine core repository (LacCore). J Paleolimnol 25:123–127. doi:10.1023/A:1008171027125

Schnurrenberger D, Russell J, Kelts K (2003) Classification of lake sediments based on sedimentary components. J Paleolimnol 29:141–154. doi:10.1023/A:1023270324800

Scholz CA, Johnson TC, Cohen AS, King JW, Peck JA, Overpeck JT, Talbot MR, Brown ET, Kalindekafe L, Gomez J, Pierson J (2007) East African megadroughts between 135 and 75 thousand years ago and bearing on early-modern human origins. Proc Natl Acad Sci U S A 104:16416–16421. doi:10.1073/pnas.0703874104

Scholz C, Cohen A, Johnson T, King J, Talbot M, Brown E (2011) Scientific drilling in the great rift valley: the 2005 Lake Malawi scientific drilling project—an overview of the past 145,000years of climate variability in Southern Hemisphere East Africa. Palaeogeogr Palaeoclimatol Palaeoecol 303:3–19. doi:10.1016/j.palaeo.2010.10.030

Shala S, Helmens K, Jansson K, Kylander M, Risberg J, Löwemark L (2014) Palaeoenvironmental record of glacial lake evolution during the early Holocene at Sokli, NE Finland. Boreas 43:362–376. doi:10.1111/bor.12043

Simonneau A, Doyen E, Chapron E, Millet L, Vannière B, Giovanni C, Bossard N, Tachikawa K, Bard E, Albéric P, Desmet M, Roux G, Lajeunesse P, Berger J, Arnaud F (2013) Holocene land-use evolution and associated soil erosion in the French Prealps inferred from Lake Paladru sediments and archaeological evidences. J Archaeol Sci 40:1636–1645. doi:10.1016/j.jas.2012.12.002

Stansell N, Abbott M, Rull V, Rodbell D, Bezada M, Montoya E (2010) Abrupt Younger Dryas cooling in the northern tropics recorded in lake sediments from the Venezuelan Andes. Earth Planet Sci Lett 293:154–163. doi:10.1016/j.epsl.2010.02.040

Stansell N, Rodbell D, Abbott M, Mark B (2013) Proglacial lake sediment records of Holocene climate change in the western Cordillera of Peru. Quat Sci Rev 70:1–14. doi:10.1016/j.quascirev.2013.03.003

Tjallingii R, Röhl U, Kölling M, Bickert T (2007) Influence of the water content on X-ray fluorescence core scanning measurements in soft marine sediments. Geochem Geophys Geosyst 8:Q02004. doi:10.1029/2006GC001393

Turner TE, Swindles G, Roucoux K (2014) Late Holocene ecohydrological and carbon dynamics of a UK raised bog: impact of human activity and climate change. Quat Sci Rev 84:65–85. doi:10.1016/j.quascirev.2013.10.030

Unkel I, Björck S, Wohlfarth B (2008) Deglacial environmental changes on Isla de los Estados (54.4°S), southeastern Tierra del Fuego. Quat Sci Rev 27:1541–1554. doi:10.1016/j.quascirev.2008.05.004

Unkel I, Fernandez M, Björck S, Ljung K, Wohlfarth B (2010) Records of environmental changes during the Holocene from Isla de los Estados (54.4°S), southeastern Tierra del Fuego. Glob Planet Change 74:99–113. doi:10.1016/j.gloplacha.2010.07.003

Van Daele M, Moernaut M, Silversmit G, Schmidt S, Fontijn K, Heirman K, Vandoorne W, De-Clercq M, Van Acker A, Woolf C, Pino M, Urrutia R, Roberts SJ, Vincze L, De Batiste M (2014) The 600 yr eruptive history of Villarrica Volcano (Chile) revealed by annually laminated sediments. Geol Soc Am Bull 126:481–498. doi:10.1130/B30798.1

Vogel H, Zanchetta G, Sulpizio R, Wagner B, Nowaczyk N (2010) A tephrostratigraphic record for the last glacial-interglacial cycle from Lake Ohrid, Albania and Macedonia. J Quat Sci 25:320–338. doi:10.1002/jqs.1311

Wastegård S, Veres D, Kliem P, Hahn A, Ohlendorf C, Zolitschka B (2013) Towards a late quaternary tephrochronological framework for the southernmost part of South America—the Laguna Potrok Aike tephra record. Quat Sci Rev 71:81–90. doi:10.1016/j.quascirev.2012.10.019

Weltje GJ, Tjallingii R (2008) Calibration of XRF core scanners for quantitative geochemical logging of sediment cores: theory and application. Earth Planet Sci Lett 274:423–438. doi:10.1016/j.epsl.2008.07.054

Wilhelm B, Arnaud F, Sabatier P, Magand O, Chapron E, Courp T, Tachikawa K, Fanget B, Malet E, Pignol C, Bard E, Delannoy J (2013) Palaeoflood activity and climate change over the last 1400 years recorded by lake sediments in the north-west European Alps. J Quat Sci 28:189–199. doi:10.1002/jqs.2609

Wohlfarth B, Veres D, Ampel L, Lacourse T, Blaauw M, Preusser F, Andrieu-Ponel V, Kéravis D, Lallier-Vergès E, Björck S, Davies S, Beaulieu J-L, Risberg J, Hormes A, Kasper H, Possnert G, Reille M, Thouveny N, Zander A (2008) Rapid ecosystem response to abrupt climate changes during the last glacial period in western Europe, 40–16 ka. Geology 36:407–410. doi:10.1130/G24600A.1

Yancheva G, Nowaczyk N, Mingram J, Dulski P, Schettler G, Negendank J, Liu J, Sigman D, Peterson L, Haug G (2007) Influence of the intertropical convergence zone on the East Asian monsoon. Nature 445:74–77. doi:10.1038/nature05431